Glacial lake outburst flood hazard under current and future conditions: first insights from worst-case scenarios in a transboundary Himalayan basin

Simon K. Allen[1,2], Ashim Sattar[1], Owen King[3], Guoqing Zhang[4,5], Atanu Bhattacharya[3,6], Tandong Yao[4,5], Tobias Bolch[3]

[1]Department of Geography, University of Zurich, Zurich, CH-8057, Switzerland
[2]Institute for Environmental Science, University of Geneva, CH-1205, Geneva
[3]School of Geography and Sustainable Development, University of St Andrews, St Andrews, KY16 9AL, UK
[4]Key Laboratory of Tibetan Environmental Changes and Land Surface Processes, Institute of Tibetan Plateau Research, Chinese Academy of Sciences (CAS), Beijing, China
[5]CAS Center for Excellence in Tibetan Plateau Earth Sciences, Beijing, China
[6]Department of Remote Sensing & GIS, JIS University, Kolkata 700109, India

Correspondence to: Simon K. Allen (skallenz@gmail.com)

Abstract

Glacial lake outburst floods (GLOFs) are a major concern throughout High Mountain Asia, where societal impacts can ~~be far-reaching.~~ extend far downstream. This is particularly true for transboundary Himalayan basins, where risks are expected to further increase as new lakes develop. Given the need for anticipatory approaches to disaster risk reduction, this study aims to demonstrate how the threat from a future lake can be feasibly assessed along-side that of worst-case scenarios from current lakes, and how this information ~~can feed practically into decision-making and response planning~~is relevant for disaster risk management. We have focused on two ~~well-known~~previously identified dangerous lakes (Galongco and Jialongco), comparing the ~~consequences~~ timing and magnitude of simulated worst-case outburst events from these lakes both in the Tibetan town of Nyalam and downstream at the border with Nepal. In addition, a future scenario has been assessed, whereby an avalanche-triggered ~~outburst~~ GLOF was simulated for a potential large new lake forming upstream of Nyalam. Results show that large (> 20 mil m^3) rock and/or ice avalanches could generate GLOF discharges at the border with Nepal that are more than 15 times larger than what has been observed previously, or anticipated based on more gradual breach simulations. For all assessed lakes, warning times in Nyalam would be only 5 – 11 minutes, and 30 minutes at the border. Recent remedial measures undertaken to lower the water level at Jialongco would have little influence on downstream impacts resulting from a very large magnitude GLOF, particularly in Nyalam where there has been significant development of infrastructure directly within the high-intensity flood zone. ~~although smallest in size, Jialongco, poses the greatest immediate threat to Nyalam and downstream communities, owing to the high potential for an ice avalanche to trigger an outburst. The future lake scenario would lead to flow depths and velocities that exceed either of the current scenarios, and the peak flood would reach Nepal up to 20 minutes faster.~~ Based on these findings, a comprehensive approach to disaster risk ~~reduction~~ management is called for, combining early warning systems with effective land use zoning and ~~capacity building~~ programs to build local response capacities. Such approaches would address the current drivers of GLOF risk in the basin, while remaining robust in the face of worst-case, catastrophic outburst events~~future emerging threat~~ sthat become more likely under a warming climate.

Keywords

Glacial lake outburst flood, process chain, hazard, risk, future, Himalaya

1 Introduction

Widespread retreat of glaciers has accelerated over recent decades in the Himalaya as in most other mountain regions worldwide as a consequence of global warming ((Bolch *et al.*, 2019; King *et al.*, 2019; Maurer *et al.*, 2019; Zemp *et al.*, 2019). A main consequence has been the rapid expansion and new formation of glacial lakes (Gardelle *et al.*, 2011; Nie *et al.*, 2017; Shugar *et al.*, 2020), which has large implications for both water resources and hazards (Haeberli *et al.*, 2016a). When water is suddenly and catastrophically released, Glacial Lake Outburst Floods (GLOFs) can devastate lives and livelihoods up to hundreds of kilometres downstream (Carrivick and Tweed, 2016; Lliboutry *et al.*, 1977). This threat is most apparent in the Himalaya, where glacial lakes have been increasing rapidly in both size and number (~~Gardelle *et al.*, 2011;~~ Zhang *et al.*, 2015; Wang et al. 2020; Chen et al. 2021), and where a ~~high~~ frequency of 1.3 GLOFs per year ~~have~~ has been recorded since the 1980s (~~Harrison *et al.*, 2018; Nie *et al.*, 2018;~~ Veh *et al.*, 2019). The fact that GLOFs can extend across national boundaries exacerbates the challenges for early warning or other risk reduction strategies, particularly in politically sensitive regions (Allen *et al.*, 2019; Khanal *et al.*, 2015a).

Lakes can develop either underneath (subglacial), at the side, in front (proglacial), within (englacial), or on the surface of a glacier (supraglacial), with the dam being composed of ice, moraine, or bedrock. In Asia, m~~M~~ost scientific attention has focussed upon the hazard associated with the catastrophic failure of moraine-dammed lakes, and particularly those trapped behind proglacial moraines (e.g., Fujita *et al.*, 2013; Westoby *et al.*, 2014; Worni *et al.*, 2012). Such lakes can be very large, with volumes ~~of up to~~larger than 100 million m^3 (Zheng *et al.* 2021b), and depths exceeding 200 m (Cook and Quincey, 2015), and are susceptible to a range of failure mechanisms owing to the low material strength of~~ ~~ the dam structure (Clague and Evans, 2000; Korup and Tweed, 2007). In Asia, as elsewhere in the world, displacement waves generated from large impacts of ice or rock have contributed to the majority of moraine dam failures, occurring predominantly over the warm summer months (Emmer and Cochachin, 2013; Liu *et al.*, 2013; Richardson and Reynolds, 2000). ~~GLOFs have proven particularly common in Tibet, with at~~ At least 17 GLOF disasters (causing loss of life or infrastructure) have been documented in Tibet since 1935, mostly originating in the central-eastern section of the Himalaya (Nie *et al.*, 2018). Coupled with rapidly increasing population and infrastructural development in the region, an urgent need for authorities to take action and implement timely risk reduction measures has been acknowledged (Wang and Zhou, 2017), considering the best available knowledge on existing threats (e.g., Allen *et al.*, 2019; Wang *et al.*, 2015a, 2018), but also with a view to the future (Furian *et al.*, 2021; Zheng *et al.*, 2021a).

Despite no clear trend observed in GLOF activity over recent decades in the Himalaya (Veh *et al.*, 2019), the ongoing expansion of lakes towards steep and potentially destabilised mountain flanks is expected to lead to new challenges in the future with implications for hazards and risk (Haeberli *et al.*, 2016b). Based on approaches to model the possible future expansion and development of new lakes (Linsbauer *et al.*, 2016) several studies have aimed to quantify the possible implications for GLOF frequency and/or magnitude for different regions (Allen *et al.*, 2016; Emmer *et al.*, 2020; Magnin *et al.*, 2020). For example, in the Indian Himalayan state of Himachal Pradesh, Allen et al. (2016) demonstrated a 7-fold increase in the probability of GLOF triggering and a 3-fold increase in the downstream area affected by potential GLOF paths under future deglaciated conditions. Meanwhile, Zheng et al. (2021a) have elaborated such analyses for the entire High Mountain Asia, revealing ~~an almost 3-fold increase in GLOF risk and the emergence of new hotspots of risk over the course of the 21st century. Significantly,~~that the number of lakes posing a transboundary threat within border areas of China and Nepal could double in the future~~, particularly within the eastern Himalayan region~~ (Zheng *et al.*, 2021a). While such large-scale, first-order studies are important for raising general awareness of the future challenges that mountain regions will face (Hock *et al.*, 2019), there are limitations in the extent to which these studies can directly inform planning and response actions at the ground level.

The need for forward-looking, anticipatory approaches to hazard and risk modelling, including attention to possible worst-case scenarios is clearly recognised within ~~recent~~ international guidelines on glacier and permafrost hazard assessment (GAPHAZ, 2017)~~, yet~~. However, practical examples on how to ~~integrate~~ account for worst-case scenarios and future lake development ~~for~~ in local GLOF hazard assessment and risk management ~~are lacking~~have been rarely demonstrated. International best practice is framed by both a first-order assessment undertaken at large scales (to identify potentially critical lakes), followed by a detailed assessment for these lakes using numerical models to simulate downstream flood intensities as a basis for hazard mapping (GAPHAZ, 2017). This is a common approach for existing threats, where the time, data, and expertise needed to invest in comprehensive hazard modelling and mapping can be well justified for a lake that is ~~determined~~ known to be critical, yet, worst-case scenarios are often neglected and may far exceed historical precedence. ~~However, f~~For future lakes, where the ~~formation of the~~timing of lake formation ~~and its eventual dam characteristics remain~~is typically highly uncertain, there remains a methodological gap in the hazard assessment process, as authorities are unlikely to undertake sophisticated hazard mapping for a threat that may not even eventuate. In this study we aim to address ~~this~~ these gaps, by providing an illustrative example of how a ~~the threat of a~~worst-case outburst scenario from a potential future lake can be ~~feasibly~~ systematically assessed along-side ~~that of~~the threat posed by current lakes, ~~and how this~~before discussing the relevance of such an assessment ~~information can feed practically into decision-making and response planning~~for disaster risk management in a transboundary context.

Focusing on the transboundary Poiqu river basin in the central Himalaya, the specific objectives of the study are to 1) apply ~~hydrodynamic modelling and~~ systematic criteria to establish worst-case outburst scenarios and assess the magnitude ~~and likelihood of worst-case outburst events~~ of downstream impacts from two potentially critical lakes, considering also the effect of recent remedial measures at one of the lakes ~~in the Poiqu river basin~~, 2) compare the results with a potential outburst from a large lake that is anticipated to develop in the future, and 3) discuss the implications for early warning or other risk reduction strategies. ~~This study is intended to provide timely input to the scoping and design phase of future GLOF risk reduction strategies in the Poiqu basin, to ensure early warning systems and other measures remain suitable under possible future scenarios.~~

2 Study area

This analysis focuses on a ca. 40 km stretch of the lower Poiqu river basin originating from Galongco glacial lake, considering potential GLOF impacts in Nyalam town (capital of Nyalam county, Tibetan Autonomous Region), and downstream to the border with Nepal at Zhangmu (Fig. 1). The elevation range of the study area extends over 6000 metres, from the summit of Shishapangma at 8,027 m a.s.l, whose glacierised slopes feed Galongco, to 2000 m a.s.l in the river valley at Zhangmu. According to Wang and Jiao (2015), mean annual air temperature and mean annual precipitation in Nyalam (3810 m asl) are 3.8°C and 650.3 mm respectively, with sub-zero temperatures lasting from November – March each year. Temperatures peak in July (10.8°C), while highest average precipitation ~~rates~~ totals are recorded in September (87.9 mm~~/month~~). In total, 60% of the annual rainfall falls during the monsoon months of July – September (Wang *et al.*, 2015b)

The Poiqu basin is the Tibetan portion of the large transboundary Poiqu/Bhote Koshi/Sun Koshi River Basin, along which the economically important Friendship Highway links China to Nepal, and where significant hydropower resources are located (Khanal *et al.*, 2015b). Based on a larger study across Tibet, the Poiqu basin has been identified as a clear hotpot of transboundary GLOF danger (Allen et al. 2019 – Fig. 1), where at least 6 major GLOF events reported over the past century, including repetitive events from Jialongco in 2002 (Chen *et al.*, 2013), and Cirenmaco in 1964, 1981 and 1983 (Wang *et al.*, 2018). The 1981 event resulted in numerous fatalities, and estimated losses of up to US$4 million (currency value as of 2015) as a result of damage to houses, roads, hydropower, and disruption to trade and transportation services (Khanal *et al.*, 2015a). Meanwhile, an outburst of 1.1 × 10^5 m^3 from Gongbatongshacuo (adjacent to Cirenmaco) in July 2016, resulted in significant damage to hydropower and roads, exacerbating losses inflicted one year earlier by the Gorka earthquake (Cook *et al.*, 2018). Whereas Gongbatongshacuo has completely drained, Cirenmaco remains a ~~large and~~ persistent threat, ~~considered~~ identified by multiple studies as being one of the most dangerous lakes in Tibet (Allen *et al.*, 2019; Wang *et al.* 2015a; Wang *et al.*, 2018).

In the current study, we focus not on Cirenmaco, which has already been the subject of comprehensive investigations (Wang *et al.*, 2018), but rather on two other well-documented threats of Jialongco and Galongco, owing to their potential to cause damage to the Tibetan county capital of Nyalam, and downstream in Nepal (Allen *et al.* 2019; Shresta et al. 2010). In fact, after Cirenmaco, Galongco and Jialongco were ranked 2nd and 3rd respectively in a recent assessment of most dangerous glacial lakes across Tibet, owing to both the physical characteristics of the lakes and their surroundings (see section 4.1), and high levels of exposure in downstream areas (Allen et al. 2019). Both moraine-dammed proglacial lakes have expanded rapidly over the past decades, with Galongco, the largest lake in the basin, increasing its area by 450% from 1.00 to 5.46 km^2 in the period 1964-2017 (Wang *et al.*, 2015b; Zhang *et al.*, 2019)~~-~~. The potential future lake is located around 6 km further upstream from Jialongco (Fig. 1 – see 3.1 for further description).

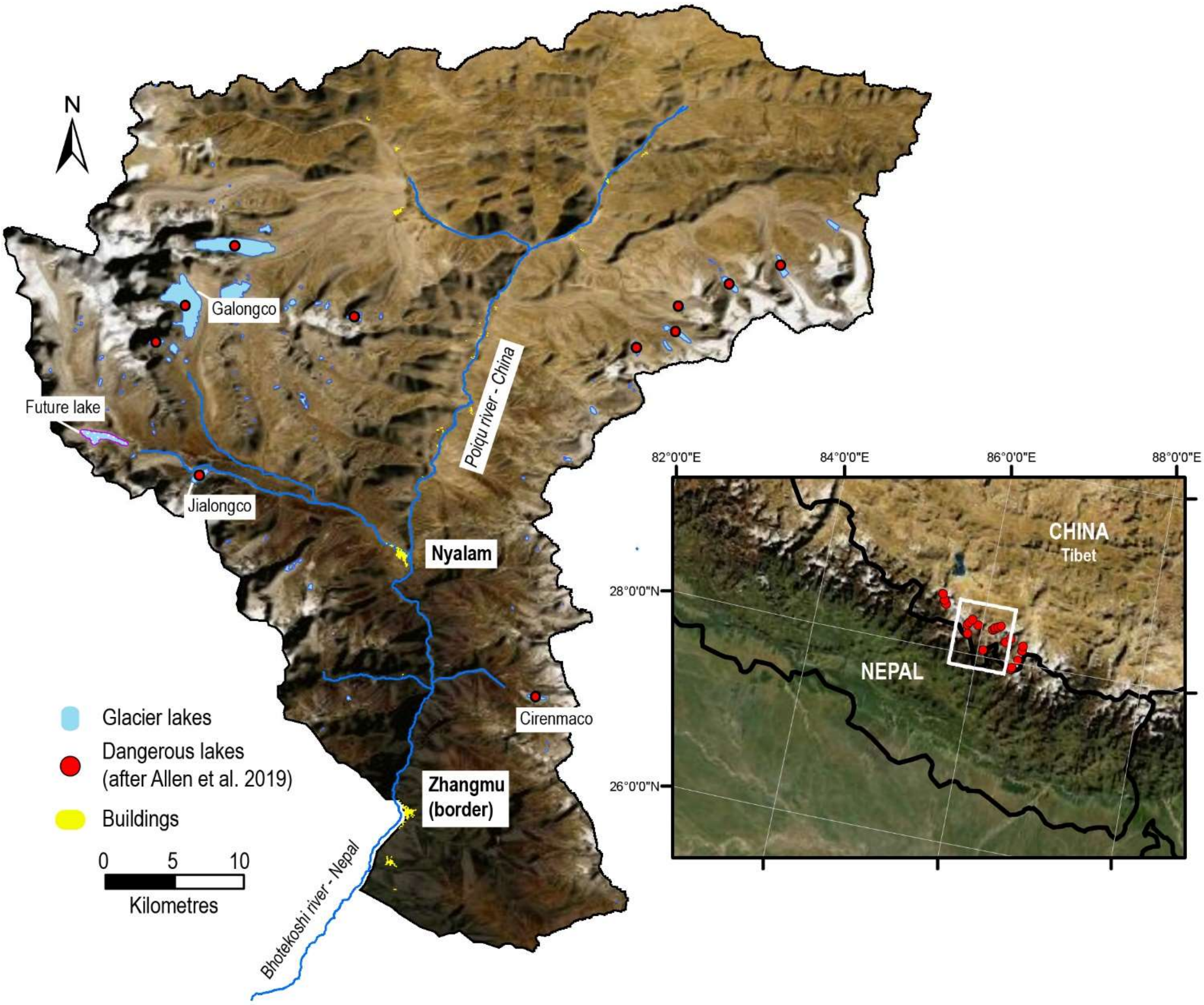

Figure 1: Location of the Poiqu River basin within a hotspot of GLOF risk, as determined on the basis of 30 potentially most dangerous lakes identified across Tibet (after Allen et al. 2019). The current lakes focussed on in this study of Galongco and Jialongco are indicated, as is the modelled future lake, the county capital town of Nyalam, and ~~border~~the town of Zhangmu, through which the border between China and Nepal passes. Cirenmaco, from which several outburst floods have been reported, is also indicated; Background image: ESRI Basemap Imagery.

3 Methodological approach

In line with recent international guidance in GLOF hazard assessment (GAPHAZ 2017), in this study we consider lake susceptibility, which determines the likelihood of a given outburst scenario to occur, and use the GIS-based open-source numerical simulation tool r.avaflow ~~hydrodynamic modelling~~ to model the GLOF process chain and determine downstream impacts. In order to compare the threat posed by the two current lakes with a ~~future~~ anticipated future lake, we focus on worst-case scenario modelling – that is to say, ~~the maximum outburst volume that could be produced from~~very large avalanche-triggered outburst events from Jialongco, Galongco, and the anticipated future lake.

3.1 Lake susceptibility and scenario development

The assessment follows a systematic approach that considers wide-ranging atmospheric, cryospheric and geotechnical factors that can influence lake susceptibility, and thereby the likelihood of a GLOF event occurring (after GAPHAZ 2017). We draw on remotely sensed data to the extent possible, complimented with field observations to enable a semi-quantitative assessment and comparison of susceptibility factors across the three lakes. Topographic characteristics (dam geometry, slope angles etc) and geological structures of the surrounding slopes were precisely measured using a high resolution 1m Pleiades imagery and Digital Elevation Model (DEM), generated from 0.5 m resolution tri-stereo Pleiades orthoimagery acquired in October 2018, covering the whole Poiqu basin. Potentially unstable zones of glacial ice were identified in the imagery and Google Earth, based on orientation and density of crevassing, with a subsequent estimate of the ice thickness and volume provided from ~~the~~ GlabTop model output (Table 1). Furthermore, the time series of Google Earth imagery was examined to identify any evidence of historical mass movements, that could indicate an enhanced threat to the lakes below. Factors assessed, their primary attributes, and sources used are further described in Section ~~XX~~4.1. Based on this assessment, and the recognition of a large ice and/or rock avalanche triggered GLOF process-chain being the most significant threat to all 3 lakes, avalanche source areas were identified as input to the process chain modelling (Table 1).

Table 1: Input scenarios for rock/ice avalanche starting zones (see Fig. 2) threatening Jialongco (JC), Galongco (GC), and the Future Lake (FL). Source area is defined based on high-resolution satellite imagery. Mean ice thickness and resulting ice volume is based on GlabTop. Note that JC-L scenario is defined for a lowered Jialongco lake, as the lake level was lowered since 2018; See Section 4.1 for further details.

	Mean slope (°)	Area (m²)	Type	Mean ice thickness (m)	Ice volume (10^6 m^3)	Mean rock thickness (m)	Rock volume (10^6 m^3)	Total volume (10^6 m^3)
JC	35	600,000	Ice avalanche	30	18 (100%)	–	–	18
JC-L	35	600,000	Ice avalanche	30	18 (100%)	–	–	18
GC	50	460,000	Rock-ice avalanche	10	4.6 (20%)	40	18.4 (80%)	23
FL	55	516,000	Rock avalanche	–	–	40	20.6 (100%)	20.6

3.~~1~~ 2 Avalanche and GLOF Modelling

The GLOF process chain was simulated with r.avaflow (Mergili et al., 2017; Pudasaini and Mergili, 2019~~; Mergili and Pudasaini, 2020~~), a GIS-based open-source simulation framework for multi-phase mass flows, which has the capacity to dynamically compute the interaction between triggering landslides (in this case rock/ice avalanches) and lakes. The model is also capable of computing debris flow hydraulics. Major model inputs ~~Apart from~~ include the initial avalanche ~~scenarios~~source characteristics (Table 1), terrain data, friction parameters and erosion parameters (see below), ~~the other major model inputs are the~~ lake bathymetry and volume.

Bathymetry surveys of Jialongco and Galongco were undertaken in 2019, using an unmanned vessel. The onboard GPS system achieves ~2.5 m horizontal positioning accuracy, while the single~~l~~-beam sonar sounder has a vertical accuracy of 1 cm ± 0.1% of depth measured. Contour maps of lake depths were interpolated by using Kriging geo-statistics. Maximum depths of 134 and 200 metres were recorded for Jialongco and Galongco respectively, while volumes based on the interpolated bathymetry were 40 and 590 x 10^6 m^3. Following the construction of an artificial channel and associated lowering of the water level in Jialongco, bathymetry was remeasured in 2021, giving a post-lowering maximum depth of 113 m, and volume of 23.5 x 10^6 m^3.

~~The total volume of water potentially released during a GLOF event is of critical importance for hydrodynamic modeling of a GLOF scenario (Westoby *et al.*, 2014). In this study, the volumes for Jialongco and Galongco were estimated by multiplying mapped lake area (A) by estimated mean depth (D_m), where D_m is calculated according to the empirical relationship of Fujita et al. (2013) which has been established based on lake data from the Himalayan region:~~

~~$D_m = 55A^{0.25}$ (1)~~

~~where A and D_m are the lake area (km^2) and mean depth (m). Lake area was mapped using Google Earth imagery from 2019.~~ For GLOF modelling ~~of~~ from the future lake, the location ~~and maximum~~ , bathymetry, and volume of the potential lake upstream from Jialongco is based on a modelled overdeepening in the glacier bed topography using GlabTop (Linsbauer *et al.*, 2012). The model is now well established for providing a first-order indication of where lakes may develop in the future (e.g., Allen *et al.*, 2016; Haeberli *et al.*, 2016a; Linsbauer *et al.*, 2016; Magnin *et al.*, 2020). The ice thickness distribution from GlabTop is subtracted from a surface DEM to obtain the bed topography, i.e. a DEM without glaciers, from which overdeepenings in the glacier bed can be detected and volumes estimated. Inputs to the model include manually edited glacier branch lines, and a DEM – in this case the NASA Shuttle Radar Topography Mission (SRTM) Version 3.0 (void filled) was used, at 30 m resolution. While the model predicts several possible locations in the Poiqu basin where large future lakes can develop, we focussed on the largest of these lakes that threaten the town of Nyalam. Based on the modelled geometry of the overdeepening, a maximum future lake depth of 168 m, and volume of 70 x 10^6 m^3 is estimated. The modeled bedrock topography forms the lake dam, i.e., the possible deposition of moraine on top of the bedrock, creating a higher dam structure, is not considered. Likewise, in keeping with a worst-case approach, we do not consider sediment deposition into the lake, that will potentially reduce the volume and longevity of the lake (Steffen *et al.* 2022). Beyond its potential size, this overdeepening was selected owing to its position in an area of ~~the~~ low surface gradient behind a pronounced terminal moraine, beneath a tongue where supraglacial ponds are already developing, and at an elevation that is lower than other overdeepenings in the area. All factors provide favourable preconditioning for the formation of a large proglacial lake (Frey *et al.*, 2010; Linsbauer *et al.*, 2016).

~~Based on the total estimated volume of the lakes, we then establish the potential flood volume (PFV) for each lake following the concept of Fujita et al. (2013), that assumes full incision and removal of the downstream slope of the dam (Fig 2a). Only where the height of the potential breach (h_b) is greater than the mean depth of the lake is the full release of the lake volume possible:~~

~~$\mathrm{PFV} = \min[h_b;D_m]A$ (2)~~

~~For example, in the case of Jialongco, the breach height is estimated at 40 m, which is less than the mean depth of the lake suggesting that even following full moraine incision, some water will remain in the lake (Fig 2b). The resulting PFV is therefore~~

estimated at 24.8 m^3 10^6 (40 m x 0.62 km^2). In comparison, the well documented 1981 outburst from the smaller Cirenmaco was estimated to have involved a breach height of up to 60 m and an outburst volume of 19 m^3 10^6 (Xu, 1988). In principle, dam geometries can be measured directly in Google Earth, although there can be severe distortions in the imagery in some regions and the DEM accuracy is unknown. Therefore, to achieve a higher level of accuracy, we measured h_b and other topographic parameters using spot elevations extracted from a higher resolution (1 m grid cell) Digital Elevation Model, generated from 0.5 m resolution tri-stereo Pleiades imagery acquired in October 2018, covering the whole Poiqu basin.

Subsequent breach parameters were calculated according to Froehlich (1995) for each outburst scenario:

$$B_w = 0.1803 K_o (V_w)^{0.32} (h_b)^{0.19} \qquad (3)$$

$$T_f = 0.00254 (V_w)^{0.53} (h_b)^{-0.9} \qquad (4)$$

where B_w is the breach width (in m), K_o is a constant which is considered to be 1.4 for overtopping failures, V_w is the volume above h_b of the lake (in m^3), and T_f (in min) is the time taken for the breach to form (where distances B_w and h_b are fully obtained).

The HEC-RAS (v 5.0.7) dam-break module was used to set up different breach scenarios for the three lakes (Table 1). Dam-break simulations were performed where the frontal moraine (dam) is defined to fail, given the calculated breach parameters (after Froehlich, 1995). Here, a progressive breach mechanism was assumed for all the scenarios where overtopping failure initiated at the crest of the moraine spreading downwards and sidewise. The outputs in the form of outflow hydrographs (discharge vs. time) were then used as boundary conditions for downstream two-dimensional GLOF routing with HEC-RAS (v 5.0.7) as far as Zhangmu (Fig 3). This hydraulic model solves the Full Saint Venant equations two-dimensionally in an unsteady flow. Two-dimensional routing requires accurate terrain information as a primary inp
Depending on the defined GLOF process-chain scenarios (Table 1), we assume the mixture of one or two solid phases in the initial avalanche (rock component; ρ=2700 kg/m³ and ice component; ρ=900 kg/m³) and one fluid phase; ρ=1000 kg/m³ (lake water), where the ice-rock volume ratios are calculated based on assessment in Section 34.1. We define the damming moraine of the lakes as entrainment zones composed of the rock phase (representing glacier deposits) with a grain density of 2700 kg/m³. A simplified entrainment model is applied, which is a product of the flow momentum and the empirical entrainment coefficient (Mergili *et al.*, 2017). However, the final erosion depths are dependent on the momentum of the particular process and are controlled by the entrainment coefficient. Other input parameters include basal friction angle (φ) and internal friction angle (δ) that govern the rheology of the flow. Here we set φ = 25°, δ = 10° for the initial stage of the process chain dominated mostly by mostly the solid phase, i.e., avalanche, lake impact, and moraine erosion. For the downstream process from the moraine, we set φ = 25°, δ = 1° to model the flow as a water-saturated debris flow. The domain of the model is constructed such that it completely encompasses the avalanche source areas down to the China-Nepal border. All the simulations are executed for a total duration set to 1 hour 15 minutes (4500 s) providing enough time to evaluate the GLOF propagation downstream to the border. Finally, to evaluate the flow hydraulics obtained in terms of flow depth and discharge,; we define three cross-sections along the flow channel located (i) immediately downstream of the damming moraine (ii) at Nayyalam (nearest settlement), and (iii) at the Zhangmu (China Nepal border).

It is to be noted that we assumed no entrainment of the frontal moraine in the Jailongco LoweringLowered Scenario (JC-L), as the damming moraine was lowered by up to 15 – 20 m, and armoured with concrete as a part of the engineering works performed for GLOF mitigation since 2018. For GLOFs originating from the Future Lake we evaluate the cascading impact of the flow impacting into Jialongco, located ~6 km- downstream (see Fig. 1). While several freely available DEMs were tested (e.g., ALOS PALSAR at 12. 5 m or HMA at 8 m), topographic artefacts led to modelling errors. As such, the 1-m Pleiades DEM was finally used for all simulations (based on imagery from 2018, with exception of the JC-L simulation which used an updated DEM from 2021 for the dam area). The limits of the defined computational flow area extend 500 m on either side of the central line of the flow channel. The flow domain was divided into equal grids of 30×30 m to attain numerical stability while performing unsteady flow computation of the breach hydrographs for each scenario individually. Considering the uniformity of land cover and lack of vegetation along the flow channel, a uniform Manning roughness of 0.045 was considered along the flow channel. The total computation time was set to 24 hours such that the modelled flood wave had enough time to propagate downstream even under potential low momentum conditions. The flow hydraulics (i.e. flow depth and flow velocity) were obtained for each inundated pixel. The time series of flow depth and velocity were measured at a point located at the centre of the river channel at Nyalam and Zhangmu.

3.2 Lake susceptibility assessment

The assessment follows a systematic approach that considers wide-ranging atmospheric, cryospheric and geotechnical factors that can influence lake susceptibility, and thereby the likelihood of a GLOF occurring (after GAPHAZ 2017). As a desk-based assessment, we draw on remotely sensed data to the extent possible, to enable a semi-qualitative comparison of susceptibility factors across the three lakes. Factors assessed, their primary attributes, and sources used are provided in Table 2. Topographic characteristics (dam geometry, slope angles etc) were precisely measured using the high resolution 1m DEM generated from Pleiades imagery. To establish the potential for ice and/or rock avalanche triggering, additional GIS-based analyses were undertaken. The overall likelihood of rock (or debris) avalanches triggering an outburst was calculated based on the concept of topographic potential (Allen *et al.*, 2016; Romstad *et al.*, 2009) which identifies within each lake watershed a) the potential for rock to detach (parameterized by slope angles >30°), and b) the potential for the resulting avalanche to reach the glacial lake (parameterized by overall trajectory slopes >14° (tanα = 0.25). Potentially unstable zones of glacial ice were identified in Google Earth, based on orientation and density of crevassing, with a subsequent estimate of the ice thickness and volume provided from the GlabTop model output (Table 3). Furthermore, the time series of Google Earth imagery was examined to identify any evidence of historical mass movements, that could indicate an enhanced threat to the lakes below.

3.3 Future lake development

Previous studies (Quincey *et al.*, 2007) have identified glacier surface attributes which may precondition the surface of debris-covered glaciers for supraglacial lake development. Previous studies (e.g. Quincey *et al.*, 2007; King et al., 2018) have identified glacier surface attributes which may precondition the surface of debris-covered glaciers for supraglacial lake development. Glaciers bounded by large lateral and terminal moraines which have a flat or gently sloping (<~2°), slowly flowing (<~10 m a^{-1}) main tongue commonly host networks ofare hotspots of supraglacial pond developments as surface meltwater cannot drain from the glacier surface (e.g. Quincey et al., 2007; King et al., 2018). Such pond networks expand when the mass balance of the glacier is negative and coalesce to eventually form a supraglacial lake at the hydrological base level of the glacier- the lowest point where the glacier surface intersects the terminal moraine (Figures 3 & 19 in Benn *et al.*, 2012). Large supraglacial lakes located close to the termini of debris-covered glaciers can persist for decades, over which period they expand, deepen and eventually transition to become proglacial lakes, such as Galongco and Jialongco. By examining contemporary and historical glacier surface velocity and elevation changes it is therefore, possible to identify glacier surfaces suited for surface meltwater ponding, which represent current and future sites of supraglacial lake development. To establish the possibility of lake development and the likely future trajectory of lake area growth on the parent glacier up-valley from Jialongco (RGI60-15.09475), we examined the surface velocity, rate of thinning, and the evolution of the geometry (surface slope) of the glacier in recent decades. Previous studies (Quincey *et al.*, 2007) have identified glacier surface attributes which may precondition the surface of debris-covered glaciers for supraglacial lake development. Glaciers bounded by large lateral and terminal moraines which have a flat or gently sloping (<~2˚), slowly flowing (<~10 m a^{-1}) main tongue commonly host networks of supraglacial ponds as surface meltwater cannot drain from the glacier surface. Such pond networks expand when the mass balance of the glacier is negative and coalesce to eventually form a supraglacial lake at the hydrological base level of the glacier- the lowest point where the glacier surface intersects the terminal moraine (Benn *et al.*, 2012).

We used the Pleiades DEM and glacier surface elevation change data generated by King et al. (2019) to examine the evolution of the geometry of glacier RGI60-15.09475 since the 1970s. Glacier surface slope estimates were derived by the fitting of linear regression models through 'average' (mean of 5 evenly spaced) elevation profiles of the glacier surface split into 750 m long segments (King *et al.*, 2018). We also assessed the current flow regime of the glacier using surface velocity data, which was generated through the tracking of glacier surface features visible in Sentinel 2 imagery over the period 2017-2019 (Pronk *et al.*, 2021). Examination of these parameters established that the conditions at the surface of the glacier (Fig. 7) are well suited to imminent glacial lake development considering the factors outlined by Quincey *et al.* (2007), namely low (<2˚) surface slope, negligible ice flow (<10 m a^{-1}) and sustained glacier thinning..

To investigate the likely size of such a lake in the coming decades we consider two different scenarios of glacier thinning between 2015 and 2100 and follow a similar method to that of Linsbauer *et al.* (2013) to simulate glacier thickness into the future, but employ different criteria to determine future lake area. Our first scenario is based on the assumption that the acceleration in glacier thinning in the Poiqu basin measured by King *et al.* (2019) is replicated by the year 2100. Such an increase in thinning will be driven by a further 1˚C increase in temperature by 2100 (Kraaijenbrink *et al.*, 2017), further to the ~1˚C increase in temperature which has occurred in the central Himalaya (Maurer *et al.*, 2019) since the 1970s. The second scenario is based on the premise that the increase in thinning which has occurred between 1974 and 2015 will be replicated over subsequent equivalent time periods (by 2056, 2097, etc). We extrapolated the thinning rates from King *et al.* (2019) and integrated the resulting elevation changes between 2015 and 2100. We then assumed that once the glacier surface had lowered to a height below the hydrological base level of the glacier (4890 m a.s.l.), meltwater ponding would occur and that DEM pixels with an elevation of less than this threshold represented lake area at that point in time.

4 Results

Based on the three assessed lake outburst scenarios fFor Jialongco, Galongco and the potential future lake, we focus below on results relating to the core hazard dimensions of GLOF magnitude and likelihood (or probability)the susceptibility of the lakes to produce an outburst event, and the potential magnitude of downstream impacts, as simulated under worst-case scenarios, and assess the exposure of buildings in the town of Nyalam. A full hazard and risk assessment, including a complete range of outburst scenarios and vulnerability mapping, is beyond the scope of this study.

4.1 Lake susceptibility and scenario developmentGLOF likelihood

The second susceptibility component of GLOF hazard assessment concerns establishes the likelihood or probability of an event from a given originlake, occurring considering the wide-ranging factors that can condition or trigger an outburst. The likelihood (which can be both qualitative or quantitative for some hazards) is always specific to a given magnitude and valid for a given time frame, recognising that ~~suscepetibitlity~~susceptibility can evolve over time (Allen *et al.* 2021). Based on this assessment, scenarios for hazard modelling ~~and mapping~~ can be established, including worst-case outburst scenarios as we focus on here. Taking a systematic approach (after GAPHAZ 2017), we compare the relative susceptibility of the three lakes considered in this study, considering also how this susceptibility might evolve in the future (Table 2). The table distinguishes those factors that condition and/or trigger an outburst event, while also linking to those factors that ~~can influence~~inform about possible outburst magnitudes ~~(see 4.1)~~.

Located in a transitional zone to the north of the main Himalayan divide, the upper Poiqu basin is subject to heavy rainfall during the Asian summer monsoon. With a significantly larger watershed area, Galongco is considered more susceptible to heavy rain and/or snow melt leading to high lake water levels, and under future deglaciated conditions the lake may become fed by a well-developed paraglacial stream network. However, even under these conditions, the relatively favourable dam geometry (low width to height ratio and 15 m dam freeboard) suggests that the likelihood and magnitude associated with an outburst via this triggering mechanism is low. Similarly, self-destruction via warm temperatures and melting of ground ice within the moraine dam ~~can be effectively discounted~~is extremely unlikely. Creeping permafrost features visible in the vicinity of Galongco, modeled mean annual ground surface temperature (MAGST) (after Obu *et al.* 2019) and a partially hummocky appearance of the lake dam, suggests ~~some presence of~~a strong likelihood of ~~an~~ a partially ice-cored moraine, but the huge width (> 200 m) and gentle downstream slope of the dam would make a catastrophic failure in the case of thawing extremely unlikely.

As with the majority of large glacial lakes across the Himalaya (Liu *et al.*, 2013; Richardson and Reynolds, 2000; Sattar *et al.*, 2021), the main triggering threat is considered to come from large slope instabilities, impacting into the lake. Under current conditions, Jialongco is ~~considered~~ assessed to be most susceptible to ice avalanches, given the presence of a steep, highly crevassed tongue positioned directly behind the lake (Fig. 2a). With an average slope of ~~36~~35°, ~~and~~ large transverse crevasses marking a sharp break in topography, and likely temperate conditions at the bed, full collapse of the glacier tongue (~~~20~~ 18 x 10^6 m^3) is considered a feasible worst-case scenario (Table ~~4~~1). The mass would impact the lake in a direction parallel to the longitudinal axis of the lake, leading to maximum overtopping wave heights and swashing effect~~, meaning even a partial collapse of the unstable ice mass could be sufficient to displace the full potential flood volume of the lake, irrespective of whether or not the dam is deeply incised~~. Smaller ice avalanches from this glacier have triggered GLOFs from Jialongco in 2002, at a time when the lake was less than half of its current size (Chen *et al.* 2013). ~~However,~~While climate warming is expected to increase temperatures and meltwater at the glacier bed (Kääb *et al.* 2021), ~~-~~potentially reducing the stability of the glacier, ~~further~~ warming-driven retreat of the tongue will see a reduction in the potential avalanche volume over time, and eventually, this threat will be eliminated completely as the ice retreats to a ~~point~~ flatter plateau.

In comparison, the partially debris-covered parent glacier tongue of Galongco has a gentle mean slope (18°) and uniform gradient. P~~largest p~~otential unstable ice masses threatening Galongco, from steep ice cliffs~~,~~ and hanging glaciers, are found higher up on the mountain (Fig. 2b), with estimated maximum volumes in the range of 0.1 – 1 x 10^6 m^3. Avalanches from the larger of these starting zones would strike the lake perpendicular to the longitudinal axis of the lake (from the west) meaning most of the energy from a displacement wave would be dissipated on the opposing side of the lake. ~~Steep ice cliffs located higher on the mountain slopes, including those found currently above where the future lake is expected to form, are estimated to have maximum volumes ranging from 0.1 – 1 x 10^6 m^3 (Table 4), and therefore are considered insufficient to generate the~~

~~worst-case outburst flood volumes simulated here.~~ It is a similar situation above the future lake, where small, and comparatively thin hanging glaciers are restricted to the slopes southwest of the potential lake (Fig. 2c).

Hence, a large rock or combined ice-rock avalanche is considered to be the most feasible mechanism capable of triggering ~~the maximum potential outburst~~a worst-case ~~flood volume event~~GLOF from either Galongco or the potential Future lake. The northeast-~~-~~facing slopes of Shishapangma rise nearly 3000 m above Galongco, and are likely to be mostly underlain by cold permafrost conditions. This is inferred both from the distribution of rock glaciers in the region, extending down as low as 4000 m a.s.l (Bolch *et al.* 2022), and modelled MAGST (Obu *et al.* 2019) (Table 2). However, the presence of ice cliffs and hanging glaciers can lead to thermal perturbations, and even melt conditions in otherwise very cold environment (Shugar *et al.* 2021). Based on close examination with high-~~-~~resolution imagery, a large potential starting zone extending from 6550 – 7340 m a.s.l was identified on a heavily fractured slope beneath the south ridge of Shishapangma (Fig. 2b). Here, as in the surrounding peaks, layered leucogranite sits above sillimanite gneisses with a gentle northerly dipping schistosity (Searle *et al.* 1997). The slope has been eroded and potentially oversteepened by the glacier below. Based on structures outcropping on the face, a 40 m ~~depth~~ maximum bedrock depth was assumed, while steep ice cliffs and firn covering the slope is estimated to not exceed 10 m, resulting in a combined starting volume of 23 x 10^6 m^3 (20% ice and 80% rock).

~~A greater likelihood of such an event is identified for Galongco, given the sheer size of the catchment meaning greater topographic potential for large rock failures, including from the slopes of Shishapangma rising nearly 3000 m above the lake. Similarly, t~~The potential future lake is positioned directly beneath the ice-free ~ 2000 m high eastern face of Ramthang Karpo Ri (Fig. 2c), where MAGST is in the range of -3°C - -6°C. The face is dissected by numerous vertical structures and there is evidence of several scarps from previous instabilities. A large potential source area was identified, comparable to the Galongco scenario, with scarps on the face suggesting similar maximum depths of up to 40 m, leading to a total rock avalanche volume of 20.6 x 10^6 m^3 (Table 1). ~~Given that Poiqu basin is located within a high seismic hazard zone (Shedlock *et al.*, 2000), large ice-rock avalanches of the magnitude needed to trigger a worst-case scenario from these lakes are possible, but remain extremely rare events. While displacement wave processes depend ultimately on the orientation of the incoming mass, and its interaction with lake bathymetry (Schaub *et al.*, 2015), we estimate an avalanche volume in the order of 50 million m^3 would be needed to initiate a worst-case outburst from Galongco. This estimate accounts for the relatively stable dam geometry, requiring a significant amount of the flood volume to be released in the initial overtopping wave, which, based on empirical evidence, can be estimated as being up to 10 times the incoming mass (Huggel *et al.*, 2004).~~

Even on a global scale, ice and/or rock avalanche volumes of ~~this~~ the magnitude ~~are~~ included in the scenarios here are ~~extremely~~ rare (Kääb *et al.*, 2021; Schneider *et al.*, 2011), although have occurred recently (Shugar *et al.* 2021) and prehistorically (Stolle *et al.* 2017) in the Himalaya. ~~-making this a high magnitude, but very low likelihood process chain G~~While~~iven that~~ Poiqu basin is located within a high seismic hazard zone (Shedlock *et al.*, 2000), it is notable that the 2015 Gorkha earthquake did not cause any large ice/~~-~~rock avalanches in the Poiqu basin, despite significant damage in Nyalam and along the highway to Nepal (Kargel *et al.* 2016). Hence, ~~-~~given a lack of historical large instabilities in the basin, ice/rock avalanches of the ~~of the~~ magnitude included in this study, are assessed ~~possible, but remain extremely rare events~~to be low to very low likelihood events (see also Section 5- discussion). Geologically there is little basis for distinguishing the likelihood of bedrock failures above the three lakes, and permafrost conditions are comparable (Table 2). Owing to the position of Jialongco directly beneath a steep glacier tongue, history of ice-avalanche triggered outburst events, and more unfavourable dam conditions (low freeboard, narrow width), we assess a worst-case outburst from this lake to be more likely than from Galongco under current conditions. Finally, all three lakes are or will be susceptible to instantaneous or progressive landslides occurring from the adjacent lateral moraines, most notably for Jialongco where active instabilities are clearly evident (Fig. 2a). Recent studies have shown that large lateral failures, either instantaneous or progressive, can be sufficient to initiate catastrophic process chains where dam geometries are sufficiently prone to erosion (~~Klimeš *et al.*, 2016;~~ Zheng *et al.*, 2021b).

~~Based on the assessment results, a large outburst scenario involving the maximum potential flood volume is considered most likely under current conditions to originate from Jialongco, triggered by an ice avalanche or large failure of the lateral moraine slopes. Large rock or combined ice-rock avalanches are a less likely, but potentially high magnitude trigger of an outburst from all 3 lakes considered. Given the large volume of water that would need to be displaced and breach depth that would need to occur, the probability of a worst-case scenario originating from Galongco is considered very low. The susceptibility of the potential future lake to avalanches, moraine instabilities, or rain and snowmelt, will ultimately depend on the its final dam geometry, and particularly its freeboard, which is highly uncertain from model results alone.~~

Table ~~3~~2: First-order lake assessment of wide-ranging factors determining the susceptibility of glacial lake (based on GAPHAZ 2017). Colours represent an expert assessment of high (orange), moderate (yellow), and low (green) susceptibility for each of the factors considered. No colour indicates the factors were not considered relevant for these lakes. Factors can be relevant for conditioning (con.) and/or triggering (trig.) a GLOF, and can also have an influence on outburst magnitude (mag.).

Susceptibility factors for GLOFS	Relevance			Relevant Attributes	Susceptibility			Assessment methods and sources
	Con.	Trig.	Mag.		Jialong Co	Galong Co	Future lake	
a) Atmospheric								
Temperature	+	+		Mean temperature	Increasing	Increasing	Increasing	Climate observations and projections (Ren *et al.*, 2017; Sanjay *et al.*, 2017)
				Intensity and frequency of extreme temperatures	Increasing	Increasing	Increasing	
Precipitation	+	+	+	Intensity and frequency of extreme precipitation events.	Increasing	Increasing	Increasing	
b) Cryospheric								
Permafrost conditions	+	+		State of permafrost, distribution and persistence within lake dam area and bedrock surrounding slopes	No permafrost in dam area (MAGST > 1°C). Degrading permafrost in surrounding ~~slopes~~headwalls (< -3°C).	~~Possible~~ Likely ice-cored moraine dam (MAGST -1°C. Degrading permafrost in surrounding ~~slopes~~headwalls (< -4°C).	~~No~~ Possible permafrost in dam (MAGST - 0.5 - -1°C). Degrading permafrost in surrounding headwalls (- 3°C - - 6°C)~~slopes~~.	Model-based results (Schmid *et al.*, 2015; Obu et al. 2019); Google Earth
Glacier retreat and downwasting	+		+	Enlargement of proglacial lakes, enhanced supraglacial lake formation, dam removal or subsidence	Lake currently at maximum extent. Glacier not in contact with lake.	Minimal potential for further expansion (+1%).	Lake will be actively expanding over several decades, as overdeepening emerges.	GlabTop; Landsat archive (Zhang et al. 2019); Google Earth; DEM differencing (King *et al.,* 2019)
Advancing glacier (incl. surging)	+			Formation of ice-dammed lakes	Not relevant	Not relevant	Not relevant	Google Earth
Ice avalanche potential		+	+	Steep glacier tongue or ice cliffs, crevasse density and orientation, ice geometry	High potential Steep heavily crevassed glacier ~~tounge~~tongue. Likely past events triggering a GLOF.	Moderate potential Considerable steep cliff ice and small hanging glaciers.	~~Moderate~~ Low potential. A few small hanging glaciers.	GlabTop; DEM slope analyses; Google Earth
Calving potential		+	+	Width of glacier calving front, activity, crevasse density	Glacier not in contact with lake.	Minimal potential (calving front = 300 m).	High potential (calving front = > 1km).	Google Earth
Lake size	+		+	Area, volume, and/or depth	Mean depth: ~~49~~ 64 m (lowered to 48 m)	Mean depth: ~~84~~ 108 m	Mean depth: ~~61~~ 46 m	~~Landsat-based lake area mapping (Zhang *et al,* 2019); Area/depth~~

					Volume: 40 (reduced to 23.5) x 10^6 m^3 Volume: ~~30~~23.~~3~~ 5 x 10^6 m^3	Volume: ~~459~~ 590 x 10^6 m^3	Volume: ~~94~~ 70 x 10^6 m^3	~~scaling (Fujita *et al.*, 2013),~~ Field based bathymetry; GlabTop for future lake
c) Geotechnical and Geomorphic								
Dam type	+		+	Bedrock, moraine, ice	Moraine, now partially armored.	Moraine	Moraine	Google Earth
Dam width to height ratio	+		+	Width across the dam crest relative to the dam height	4:1 (engineered now to 8:1)	9:1	8:1 (large uncertainty)	Google Earth; High resolution DEM analyses (Pleiades)
Freeboard ~~to dam height ratio~~(measured from the crest of the dam to the lake water level, irrespective of any outflow channel)	+		+	Elevation difference between lake surface and lowest point of moraine.	~ 20 m (engineered now to ~ 10)	~ 15 m	~ 10 m (large uncertainty)	Google Earth; High resolution DEM analyses (Pleiades)
Downstream slope of dam	+			Mean slope on downstream side of lake dam.	~~30°~~Artificially armored channel	10°	20° (large uncertainty)	Google Earth; High resolution DEM analyses (Pleiades)
Vegetation on dam	+			Density and type of vegetation (grass, shrubs, trees).	Partially armored. Grass/scrub ~~on downstream slope~~in other areas.	Absent	Absent	Google Earth
Catchment area	+			Total size of drainage area upstream of catchment	9 km^2	35 km^2	10 km^2	DEM analyses
Catchment mean slope	+			Steepness of catchment area	32°	28°	29°	DEM analyses
Catchment drainage density	+			Density of the stream network in catchment area	Low density stream network to develop under deglaciated conditions.	Moderate density stream network to develop under deglaciated conditions.	Low density stream network to develop under deglaciated conditions.	GIS based hydrological modelling
Catchment stream order	+			Presence of large fluvial streams, facilitating rapid drainage into lake	Low order streams to develop in future	Moderate order streams to develop in future	Low order streams to develop in future	GIS based hydrological modelling
Upstream lakes	+			Presence and susceptibility of upstream lakes.	None currently. Two small lakes (~0.01 km^2) anticipated in future.	None currently or anticipated in future.	None currently or anticipated in future.	GlabTop; Google Earth
Rock avalanche potential		+	+	Steep, structurally unstable bedrock slopes with potential to runout into the lakes.	~~TP = 3820~~ Steep, heavily fractured slopes. Recent instabilities not evident. Scarps indicative of prehistoric	~~TP = 7760~~ Steep, extensively glaciated slopes. Recent instabilities not evident. Scarps indicative of	~~TP = 3876~~ Steep, heavily fractured slopes. Recent instabilities not evident. Scarps indicative of	GIS-based topographic potential modelling; Google Earth and high resolution imagery.

					failures.~~Recent instabilities not evident. Scarps indicative of prehistoric failures.~~	prehistoric failures.~~Recent instabilities not evident. Scarps indicative of prehistoric failures.~~	prehistoric failures.	
Moraine instabilities		+	+	Potential for landslides from moraine slopes into the lake	Steep moraine and talus slopes > ~~500~~ 400 m high. Large instabilities evident.	Steep moraine slopes 100 – 200 m high. Minor instabilities evident.	Steep moraine slopes in the order of 100 – 200 m anticipated.	Google Earth
Seismicity		+		~~Potential magnitude & frequency,~~Peak ground acceleration	Very High 5.1 m/s^2	High 4.1 m/s^2	Very High 4.6 m/s^2	Global Seismic Hazard Map (Shedlock *et al.*, 2000)

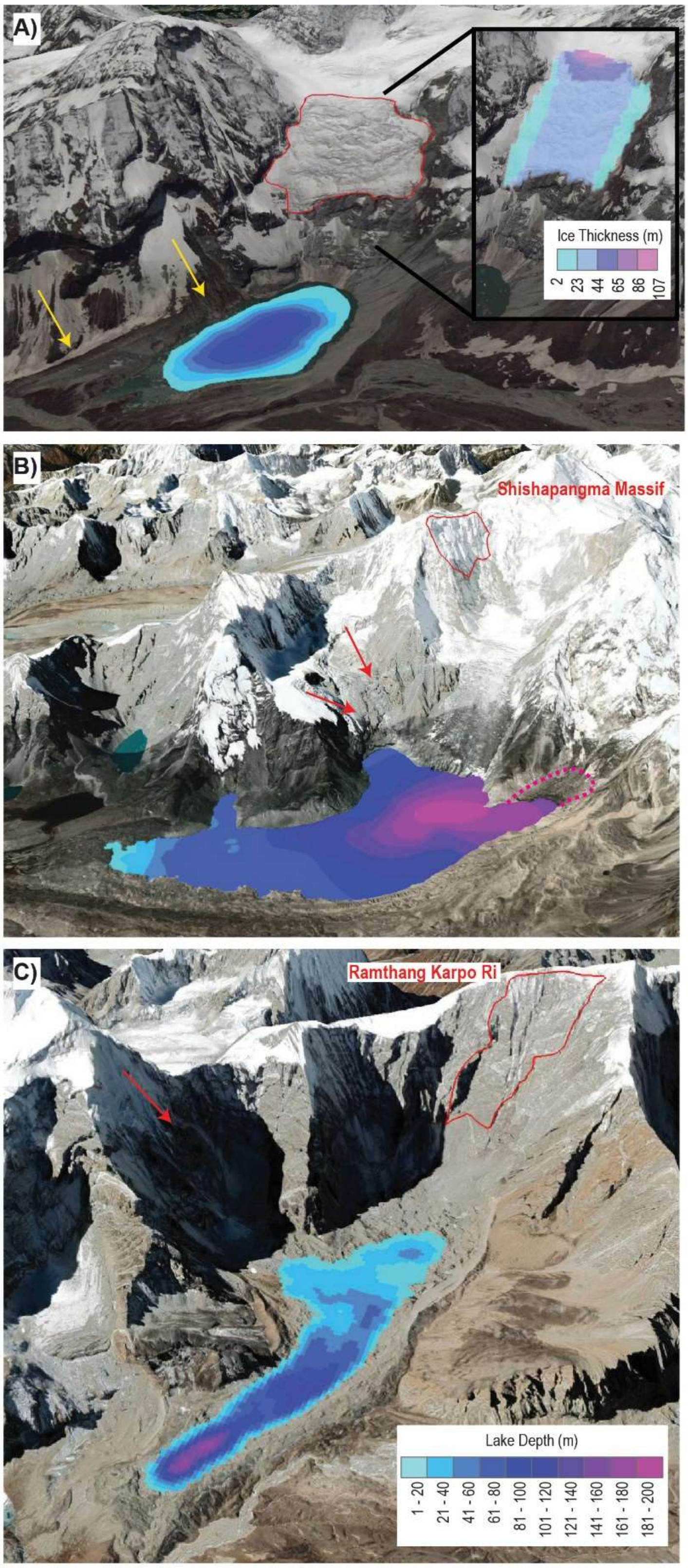

Figure 2~~5~~: ~~Primary~~ Rock/ice avalanche starting zones (in red) ~~threatening the assessed glacial lakes~~used as input scenarios for the modelling of outburst flood process chains from the 3 lakes (see Table 1 for details). A) Jialongco: The inset shows the ~~GLABTOP~~ GlabTop modelled ice thickness of the ~~main~~ ice avalanche source area, and yellow lines indicate the steep lateral moraine walls also threatening the lake (see also Figure 9). B) Galongco: Large rock/ice avalanche source area outlined in red, while arrows indicate

smaller sources areas of unstable ice, with ~~Future minimal~~possible future expansion of the lake shown by the ~~blue~~ dashed line. C) Projected ~~New~~ Future Lake: ~~GLABTOP modelled future maximum lake extent in blue~~Large rock avalanche source area outlined in red, while arrow indicates possible source area of smaller ice avalanches. Measured (and interpolated) lake bathymetry is shown in A and B, with modelled bathymetry of the future lake (C) derived from GLABTOP. Background imagery from Google Earth.

~~**Table 4: Measured and modelled dimensions of primary ice avalanche starting zones (see Fig. 1) threatening Jialonco (JC), Galongco (GC) and the Future Lake (FL). Mean ice thickness and resulting ice volume is based on GLABTOP.**~~

	Mean slope (°)	Mean ice thickness (m)	Ice area (m^2)	Ice volume (10^6 m^3)	Angle of reach (tan^{-1})
JC1	36	34	589,126	19.9	0.48
GC1	35	45	482,144	21.8	0.37
GC2	30	39	229,686	8.9	0.42
GC3	26	43	352,274	15.0	0.41
GC4	25	53	236,424	12.6	0.37
FL1	42	8	12,119	0.1	0.56
FL2	47	24	48,809	1.1	0.49
FL3	52	27	27,305	0.7	0.51

4.2 GLOF ~~impact~~modelling

Worst-case outburst scenarios for the three lakes were simulated until the border between China and Nepal (town of Zhangmu). The modeled flow does not extend beyond the border owing to the limited coverage of the required high--resolution Pleiades DEM. Of the two current lakes assessed, the modeled peak discharge from Galongco is more than ~~14~~ 5 times larger than that from Jialongco, leading to flow depths up to ~~5~~ 14 m higher ~~and velocities up to 2 m^3 s^{-1} faster~~ impacting the town of Nyalam (Table 3, Fig. 3 and 4). At the border, 20 km downstream, inundation depths are up to ~~10 times larger~~17 m higher for the Galongco ~~event~~ simulation as the ~~flow becomes~~large volume of water becomes constricted in the narrow topography of the valley, with discharge values remaining above 100,000 m^3 s^{-1} even after 1 hour (Fig. 3) ~~(Table 1, Fig. 3)~~. ~~A~~ The simulated worst-case outburst from the potential future lake~~, with a release volume of 70 x 10^6 m^3, and~~ has a calculated peak discharge at the dam of ~~42,917~~359,628 m^3 s^{-1}, ~~would~~ resulting in flow depths (~~20.1~~27 m) and ~~velocities~~ discharge (~~13.9~~163,667 m^3 s^{-1}) in Nyalam that would exceed ~~events from both~~that of Jialongco ~~and Galongco~~, but are an order of magnitude lower than from Galongco. ~~while downstream at the border, flow depths would be lower than that of the Galongco outburst (23.8 vs 27.9 m), but with significantly higher velocities (13.9 vs. 9.4 m^3 s^{-1}).~~ Differences in ~~failure time, peak velocities,~~the shape of the outflow hydrographs at the dam (Fig. 3a), and travel distance, lead to minor variations in the arrival of the modelled flood waves in Nyalam and further downstream at the border with Nepal~~, with implications for warning times and response strategies (see Discussion)~~. The flood wave from Jialongco first registers after ~~48~~ 6 minutes in Nyalam, with the maximum flow heights arriving ~~4~~ 2 minutes later (all times relative to the initial avalanche release). In contrast, the flood wave from Galongco first registers after ~~82~~ 10 minutes, with maximum flow heights arriving ~~26~~ 4 minutes later. An outburst from the potential future lake has ~~the quickest~~ a similar arrival time of only ~~42~~ 11 minutes in Nyalam, ~~reaching~~ while all simulated outbursts reach the Nepalese border within a range of 28 - 32~~0~~ minutes ~~later (compared to 40 minutes later for the existing lakes)~~after the avalanche release. Notably, the remedial measures undertaken at Jialongco, which result in a larger initial peak discharge and lower debris entrainment (due to lowering and armouring of the lake dam), result in a worst-case GLOF that attenuates at a slower rate (54% decrease in discharge between Nyalam and Zhangmu) compared to the simulation for the original lake (81% decrease in discharge between Nyalam and Zhangmu) (Fig 3).

Upstream of Nyalam a backwash effect is produced by the narrowing of the valley, extending for 600 m up the Poiqu river, with maximum flow depths of 25 m. We note that model simulations undertaken using several coarser DEMs (e.g., ALOS PALSAR at 12. 5 m or HMA at 8 m) all resulted in significant modelling artefacts in this region immediately up- and down-stream from Nyalam owing to voids in the DEMs in this area of complex topography. As a consequence, physically implausible flow depths exceeding 100 m were simulated due to artificial blockages along the river path, while the timing of the floodwave was effected by the stagnation of the flow occurring behind these blockages.

Potential processes that could significantly further enhance and/or modify the GLOF magnitude include entrainment of large volumes of sediment along the flow path leading to additional bulking of the flow volume, blockages of a river by GLOF deposits leading to secondary outburst events, and a process chain involving more than one lake. Significant erosion of sediment and a catastrophic transformation into a debris flow event is from within the main river channels is considered unlikely for any of the three outburst scenarios, given that average trajectory slope angles measured- along the flow paths (Fig. 3) are well below those needed to entrain sediment from within a channel (Huggel *et al.*, 2004). However, undercutting, In the absence of significant entrainment of sediment, there is limited potential for large deposits to block adjacent waterways, although erosion and destabilisation of the river banks as a result of the GLOFflood waters means that such secondary hazards cannot be excluded, particularly in the steep sided gorge downstream of Nyalam. Upstream ofImmediately below Nyalam, the valley narrows, leading to pooling of water in the simulations, Nyalam aand a backwash effect is produced is produced by the narrowing of the valley, extendingthat extends for 600 m 2 km up the Poiqu river, with maximum flow depths of 25>60 m under the Galongco scenario (Fig. 3a). Significant deposition of sediment can be anticipated within this backwash zone, with the potential to block the Poiqu river and form a major secondary hazard, in line with processes observed and modelled during the 2021 catastrophic mass flow in Chamoli, northern India (Shugar *et al.* 2021). We note that model simulations undertaken using several coarser DEMs (e.g., ALOS PALSAR at 12. 5 m or HMA at 8 m) all resulted in significant modelling artefacts in this region immediately up- and down-stream from Nyalam owing to voids in the DEMs in this area of complex topography. As a consequence, physically implausible flow depths exceeding 100 m were simulated due to artificial blockages along the river path, while the timing of the floodwave was effected by the stagnation of the flow occurring behind these blockages.

Table 13: Measured and modelled lake and outburst flood parameters for the three assessed lakesGalongco (GL), Jialongco pre-lowering (JC), Jialongco post-lowering (JC-L), and the future lake (FL). All timings are relative to the start of the initial rock and/or ice avalanche.

	GL	JC	JC-L	FL
Lake area (km^2)	5.46	0.62	0.49	1.54
Mean lake depth (m)	84108	4964	48	46
Lake volume (10^6 m^3)	459590	3040	23.5	70
Potential flood volume (10^6 m^3)	262	25		70
Breach height (m)	48	40		70
Breach width (m)	260	118		183
GLOF peak at dam (m^3 s^{-1})	107,802585,686	7,50792,421	101,919	42,917359,628
Time of arrival at Nyalam	82 10 min	48 5 min	6 min	42 11 min
Flow depth at Nyalam (m)	17.637	12.523	23	20.127
Flow velocity discharge at Nyalam (m^3 s^{-1})	11.6221,655	9.564,124	77,695	13.9163,667
Time of arrival at Zhangmu	128 28 min	92 32 min	28 min	72 30 min
Flow depth at Zhangmu (m)	27.929	17.47	12	23.814

Flow ~~velocity~~ discharge at Zhangmu ($m^3 s^{-1}$)	~~9.4~~170,404	~~9.2~~12,251	35,389	~~13.9~~54,656

In contrast to previous modelling results for Galongco (Shrestha *et al.* 2010; Zhang *et al.* 2021), the worst-case avalanche triggered GLOF path is not confined to the existing river channel, overtopping the orographic-right side of the valley (bounded by old moraines) and spilling over into Jialongco to form a second, larger flow path towards Nyalam (Fig. 3a). The two paths converge again about 6 km upstream from Nyalam. The hyper-elevation of the flow that enables this overtopping is consistent with observations of catastrophic mass flows of comparable magnitudes (Shugar *et al.* 2021). Results further indicate that an outburst event from the potential future lake could slam into, pool up, and eventually overtop the lateral moraine of Jialongco, producing a potential chain reaction where Jialongco also breaches (Fig. ~~4~~5). ~~Maximum flow heights measured at the surface of Jialongco reach 27 m, suggesting a significant volume of water could enter the lake via overtopping.~~ Despite adding volume to the flow, the presence of Jialongco with its prominent lateral moraine acts as a topographic obstruction that slows and reduces the energy of the outburst event, with a 50% reduction in discharge values measured immediately upstream and downstream of Jialongco. ~~Simultaneously, the outburst from upstream would lead to erosion at the front distal slope of the Jialongco dam area, as the flow is constrained in this area leading to high energy levels.~~ Although only one specific cascading lake interaction, this example highlights that lakes positioned downstream of another lake do not necessarily increase GLOF hazard, depending upon the downstream lake geometry and its orientation relative to the incoming GLOF path. ~~The combined high-impact low-probability chain reaction involving near-simultaneous breaching of the potential future lake and Jialongco requires more sophisticated modeling to fully analyse downstream impacts, but in a first approximation could lead to maximum combined flow depths >30 m in Nyalam.~~

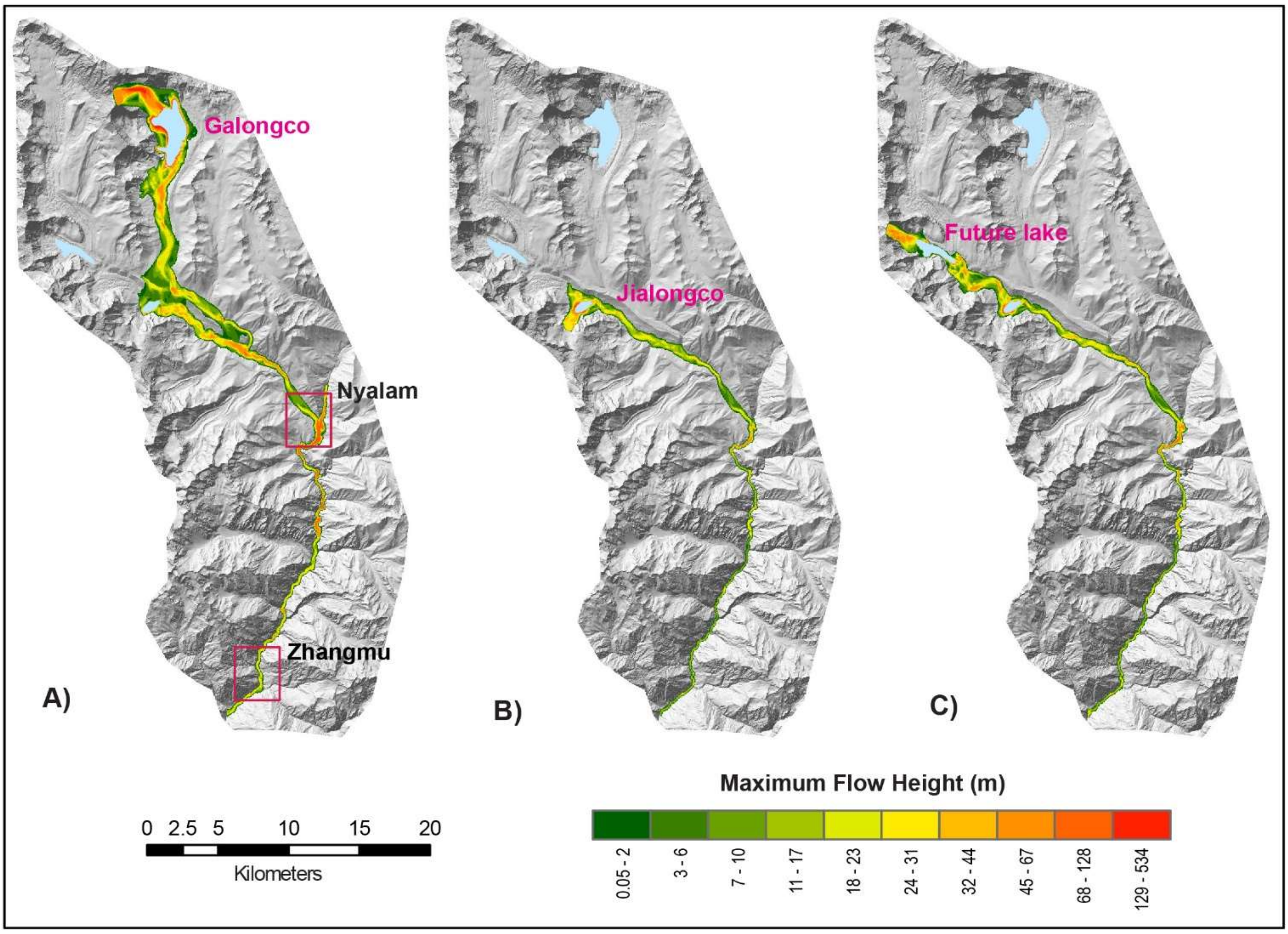

Figure 3: Modelled GLOF flow heights for worst-case scenarios from A) Galongco, B) Jialongco (JC-L), and C) the potential future lake. The location of Nyalam and Zhangmu towns are indicated by the red boxes in (A) .

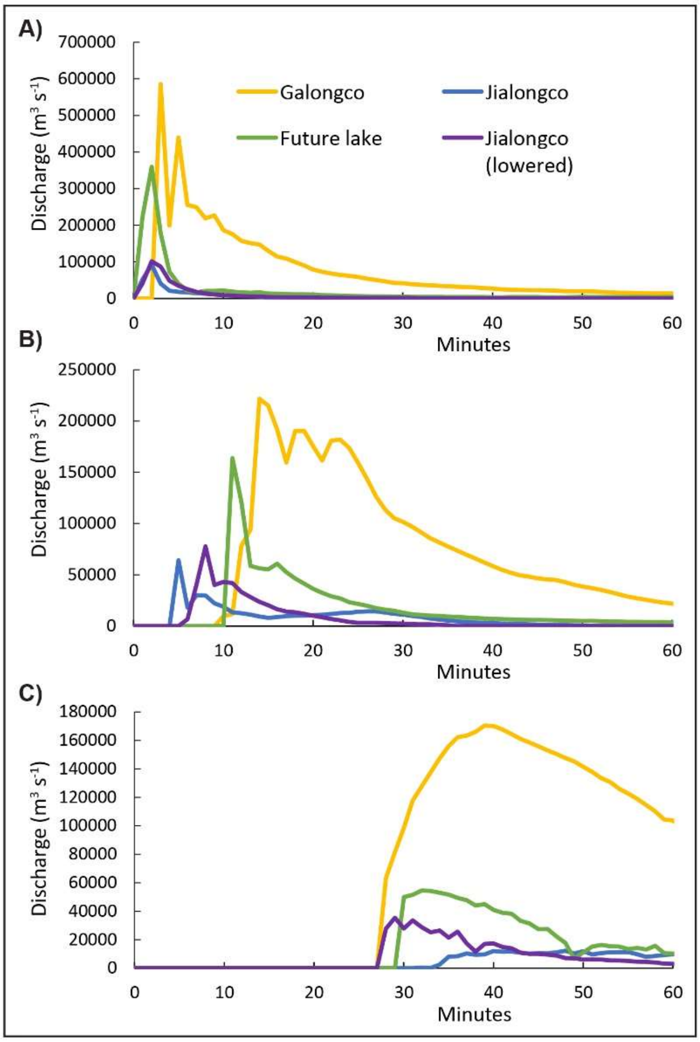

Figure 4: A) Modelled GLOF ~~flow heights for~~discharge for three assessed lakes~~.~~ taken at A) the lake dam, B) Nyalam and C) Zhangmu. ~~Numbers indicate the overall trajectory slope (tan^{-1}) for different sections along the GLOF paths. Insets B) and C) provide a time series of maximum flow height and maximum velocity measured in Nyalam and downstream at the border town of Zhangmu, respectively.~~

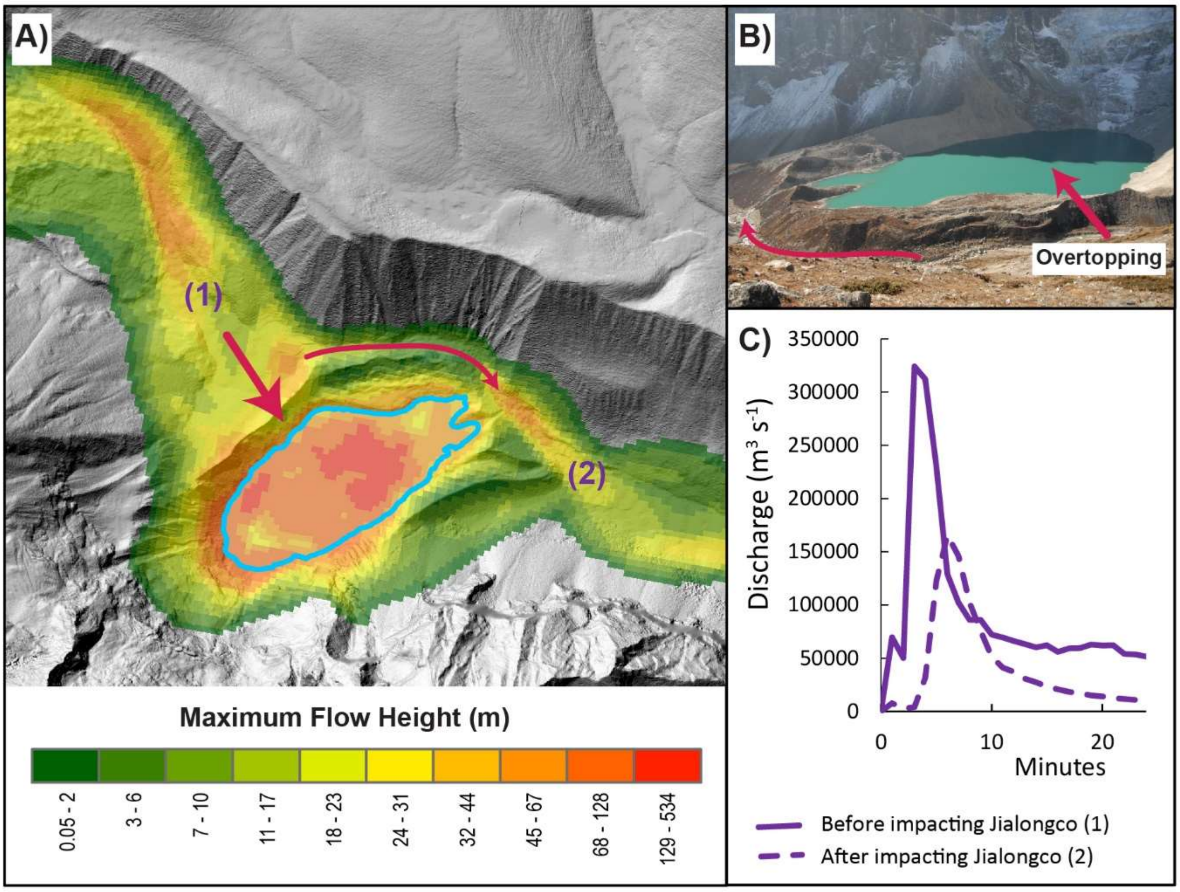

Figure 5: A) Modelled GLOF flow heights for an outburst event from the potential new lake, showing area of pooling and overtopping into Jialongco. Background DEM generated based on Pleiades data 15 Oct 2018 © CNES and Airbus DS. The moraine height at the point where overtopping is illustrated in the photo (B) is around 40 m (Photo: O. King, October 2018). C) Flow hydrographs immediately upstream (1) and downstream (2) of Jialongco are simulated with r.avaflow. Note that the simulation is based on the post-lowering lake bathymetry and dam geometry of Jialongco (JC-L). ~~Photos show the area of pooling (B), and flow concentration and potential erosion at the front of Jialongco (C). Photos: S. Allen (October 2017).~~

4.3 GLOF impact and exposure

We identify from Open Street Map and Google Earth imagery, the buildings in Nyalam exposed to different GLOF intensity levels according to simulated ~~flood flow heights~~debris flow intensities (after GAPHAZ 2017) ~~(after Pozzi *et al.*, 2005)~~. While classification schemes vary across countries, land areas potentially affected by high flood or debris flow intensities (calculated on the basis of flow heights and/or flow velocities), are typically considered as high hazard zones even for low probability events (GAPHAZ, 2017). In Nyalam, lower flow heights associated with an outburst from Jialongco result in marginally lower levels of exposure compared to simulated events from Galongco or the potential future lake (Fig. 6). Despite t~~T~~he majority of buildings in Nyalam ~~are~~ being located ~~high~~ 10 – 20 metres above the river channel, where they ~~are~~ have been unaffected by past outburst events from Jialongco (Chen *et al.* 2013), ~~safe even in in the~~there is clearly significant exposure within the high intensity zone ~~event~~ of a worst-case outburst. ~~However~~Furthermore, ~~it is clear that~~ the rapid expansion of infrastructure along the river banks north of the main settlement over the past several years has significantly increased the built area exposed to potential GLOF events, with many new buildings located in the high intensity flood zone. Overall, levels of exposure are comparable for simulated outbursts from both Galongco and the potential future lake, with both worst-case events also likely to disrupt the main ~~national road~~highway and bridges linking to the town.

Downstream from Nyalam in the reach to the border with Nepal there are few buildings located along the river bank, and the main threat is to ~~a~~ the ~~7.5~~38 km stretch of the transnational highway ~~(Fig. 4)~~, of which the proportion affected by high-intensity flood levels is ~~74~~27% and ~~96~~40%, for modelled outbursts from Jialongco and Galongco respectively (~~up to~~and ~~9~~28% for the ~~potential~~ future lake scenario). While we did not simulate beyond the border ~~owing to the limited coverage of the required high resolution Pleiades DEM~~, previous events (e.g., Cook *et al.*, 2018; Wang *et al.*, 2018), and assessment studies (Khanal *et al.*, 2015a; Shrestha *et al.*, 2010) have highlighted the significant risk to Nepalese communities, hydropower stations, and other infrastructure located along the banks of the Bhotekoshi river.

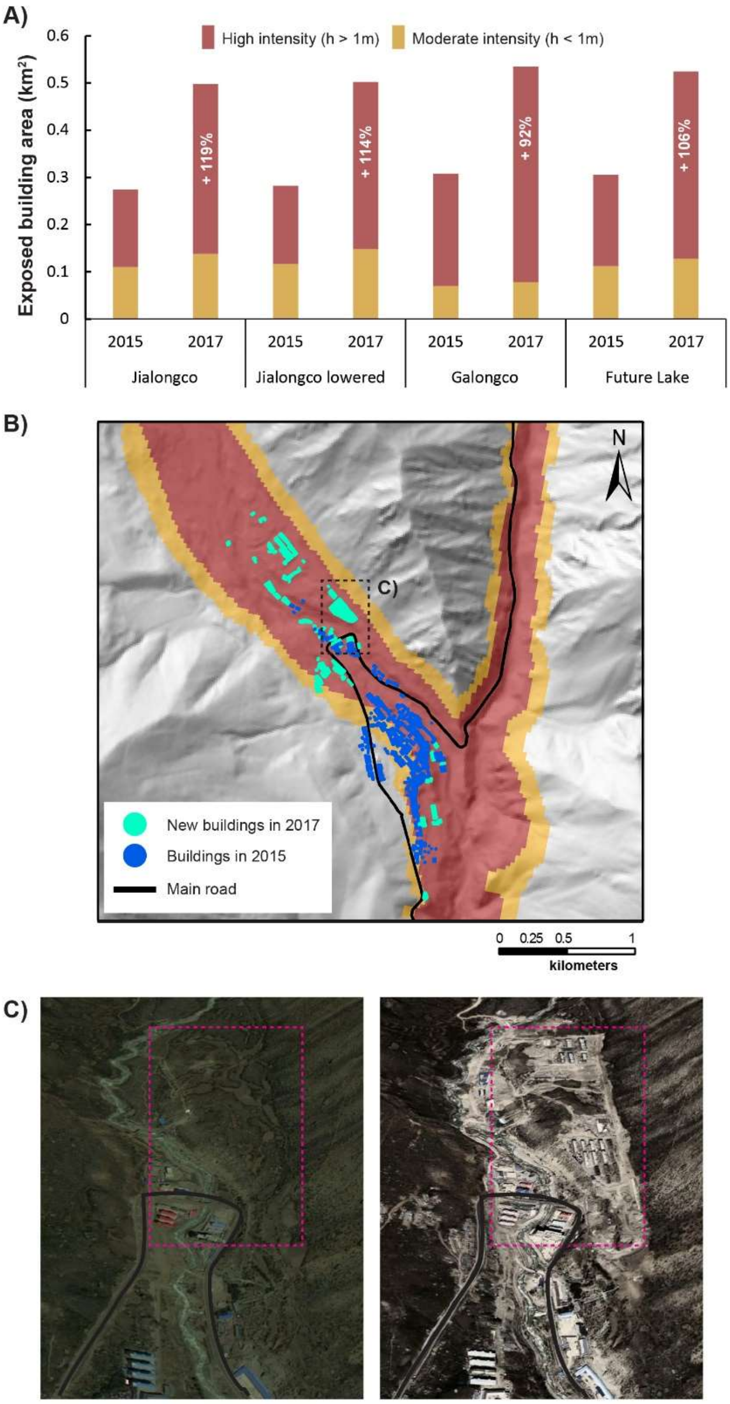

Figure 2~~6~~: A) Built area in Nyalam exposed to modelled GLOF intensity levels for the three assessed lakes, showing the effect of rapid infrastructural development between 2015 and 2017. The percentage indicates the increase in built area within the high intensity zone. B) Modelled intensities for the Galongco outburst scenario showing the recent expansion of infrastructure, as seen in Google Earth imagery (C) from June 2015 (left) and October 2017 (right). A notable area of infrastructure development just upstream of the main bridge is highlighted in the dashed rectangle.

4.4 Trajectory of future lake development

The thinning of glacier RGI60-15.09475 over at least the last four decades has caused the development of a glacier surface that is well suited for supraglacial lake development (Fig. ~~8~~7). The central 2.5 km of the glacier's ablation zone, where supraglacial ponds are already forming, is effectively stagnant, very gently sloping and has become heavily pitted due to differential ablation in response to spatially variable debris thickness. These conditions will enable the further expansion of the supraglacial pond network, which is unlikely to drain quickly.

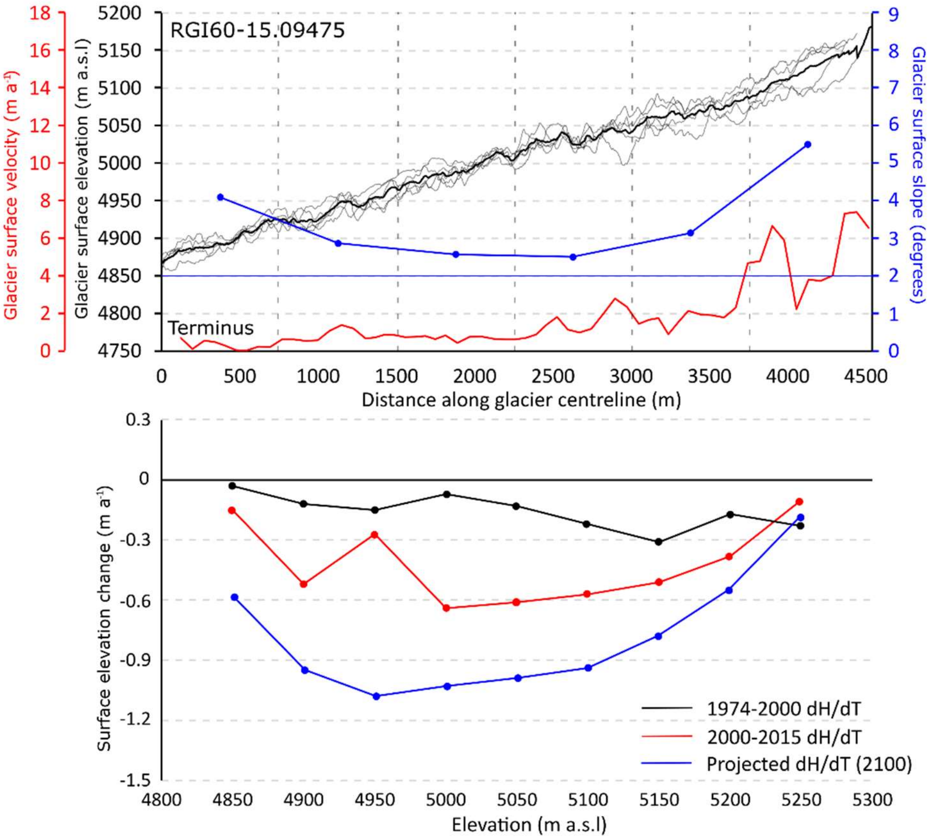

Figure 7: (A) Surface topography, slope, and velocity regime of glacier RGI60-15.09475 in 2017/18. Widespread meltwater ponding is expected once glacier surface slope declines to ~2° and little flow is evident to allow for crevasse formation and meltwater drainage. (B) Surface elevation change over the glacier from DEM differencing over the period 1974-2000 and 2000-2015 and the rate of elevation change projected to occur by 2100 (Scenario 1). The same gradient of thinning is assumed to occur by 2056 and be replicated again by 2097 in Scenario 2.

The extrapolation of thinning measured over the last four decades over glacier RGI60-15.09475 suggests that a large portion of the glaciers surface will soon sit below an elevation where supraglacial meltwater would normally drain from the glacier surface, allowing for the development of a supraglacial lake. Under scenario 1 (1974-2015 thinning replicated by 2100), 0.6 km^2 of the glaciers surface will be below the hydrological base level of the glacier by 2100 (Fig. 8). The majority of this area will be located within 1 km of the glacier's terminal moraine, although some small areas further up-glacier will also sit below the hydrological base level by 2100 due to the glacier's inverse ablation gradient (Fig. ~~7~~8). Under scenario 2 (1974-2015 thinning replicated by 2056, 2097), up to 1.33 km^2 of the surface of glacier RGI60-15.09475 will sit below the hydrological base level of the glacier by 2100. ~~In addition to the large area proximal to the terminus of the glacier which will sit below the hydrological base level,~~Hence, a large portion of the glacier surface above the 1.54 km^2 overdeepening identified by GlabTop (Table 3) will ~~also~~ have become susceptible to supraglacial lake expansion and proglacial lake formation by 2100 (Fig. ~~8c~~8d).

Projected thinning exceeds the ice thickness estimated by GlabTop in current ablation hotspots, most notably towards the terminus of the glacier, where the future ice surface elevation is similar to the simulated bedrock elevation by 2070 under scenario 1 and 2045 under scenario 2. Extrapolated thinning does not match the estimated ice thickness over the majority of the area of the proposed overdeepening further up glacier, where GlabTop suggests ice could be up to 230 m thick.

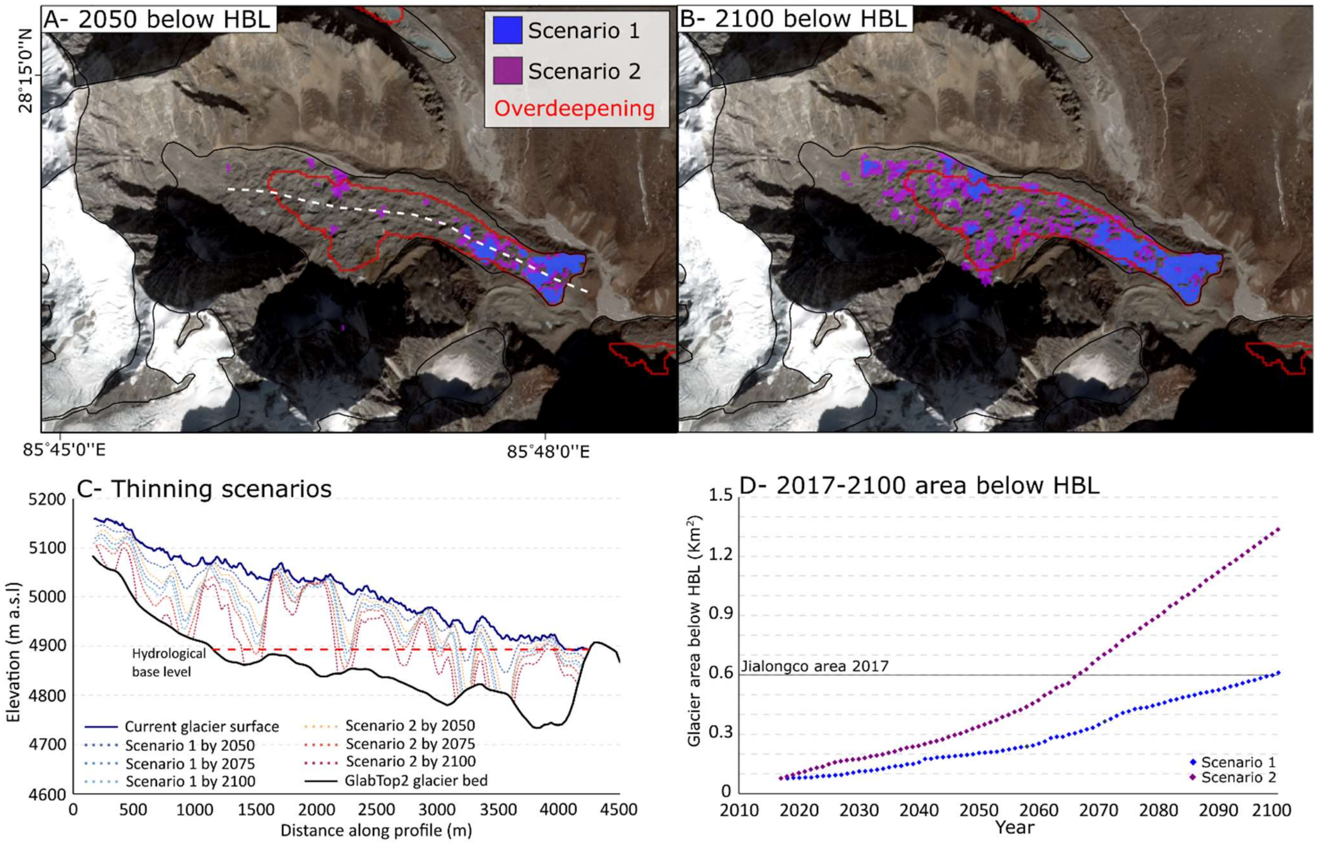

Figure 8: Meltwater ponding (if elevation < the hydrological base level of the glacier) by 2050 (A)(A), 2075 (B) and 2100 (BC) under different scenarios of thinning for glacier RGI60-15.09475. Glacier surface elevation profiles (taken along profile on panel A) under each scenario of thinning are also shown in panel C. The full timeline of supraglacial lake area expansion is shown in (D). The area within the red polygon shows the location of a bed overdeepening (1.54 km^2) predicted by GlabTop 2. Ice flow is from left to right in A-C.

5 Discussion

The results from this study demonstrate how , on the primary basis of remotely sensed datasets and GIS tools, GLOF risk hazard management planningassessment at the basin-scale can be expanded to consider new threats that may develop in the future. In doing so, this study has taken established approaches for lake susceptibility assessment (GAPHAZ 2017) and outburst GLOF modelling (Mergili *et al.* 2017)(Westoby *et al.*, 2014) and applied these approaches for the first time to consider also an outburst scenario from a potential future lake. To the extent possible, the assessment was based on freely available data and imagery. However, in steep, complex mountain topography such data can have limitations, and a high-resolution DEM derived from Pleiades imagery was required to achieve accurate GLOF modelling results for Poiqu River basin. While not intended to substitute the type of comprehensive multi-scenario modeling and field-based hazard mapping that needs to support decision-making (e.g., Frey *et al.*, 2018), the results from this study provide an intermediary step for disaster risk management planning. Using the tools and approaches demonstrated here, authorities can effectively bridge the knowledge gap between the known ~~existing~~ threats to which they ~~must immediately~~may already be responding, and those potentially much larger, yet poorly constrained threats that are anticipated to emerge or become more likely in the future.

For the Poiqu basin, these results come at an opportune time, given that local authorities over the past years ~~appear to~~ have initiated major engineering work at Jialongco (Fig. 9). In principle, the focus of authorities on Jialongco is supported by the results of this study, which indicate that the lake ~~poses the greatest immediate~~has the greatest likelihood of producing a large GLOF that threatens ~~to~~ the village of Nyalam, and, under a worst-case scenario, will lead to significant flood heights and ~~velocities~~ discharges downstream in Nepal. While assessed to be less likely, a large rock/ice-avalanche triggered outburst from Galongco would result in a higher intensity flood event, with discharge values in Nyalam almost 3 times larger than those simulated for Jialongco ~~although full drainage of the lake volume is not considered feasible. In fact, despite its rapid expansion over recent years (Wang *et al.*, 2015b; Zhang *et al.*, 2019), the maximum potential flood volume of Galongco, as limited by the dam geometry and potential height of the moraine breach, would likely not have changed~~. ~~our~~ At the border with Nepal (Zhangmu), our simulations reveal ~~a~~ potential peak discharges in the range of 35,000 – 170,000 m^3 s^{-1} under ~~a~~ worst-case scenarios ~~that is~~, which is more than ~~10~~ 15 times larger than indicated by ~~previous~~ earlier ~~modeling~~modelling studies (Shrestha *et al.*, 2010), suggesting that previously estimated potential property losses of up to US$197 million in downstream communities of Nepal are ~~a~~ far lower ~~limit to~~than what could feasibly occur. In comparison with past events, the 1981 outburst from Cirenmaco, resulting in around 200 fatalities and up to US$4 million damage, had an estimated peak discharge of around 10,000 m^3 s^{-1} in Zhangmu (Wang *et al.* 2015; Cook *et al.* 2018), while the 2016 event from Gonbatongsha lake was about half this magnitude again, but resulted in economic losses of > US$ 70 million, but no loss of life (Sattar *et al.* 2022).

Despite the threat the lake poses, the focus at Jialongco on hard engineering strategies to reduce GLOF risk could prove both costly and inefficient, if not complimented by a more comprehensive and forward-looking strategy that considers large process chains and appropriate response actions. ~~Although the overall strategy of authorities is not clear, the recent~~The removal and armouring of much of the frontal moraine and ~~apparent enhancement~~ construction of ~~the~~ a stable outlet channel (Fig. 9) ~~has had~~would have only a minimal effect on the potential downstream ~~flood~~GLOF magnitudes resulting from a catastrophic ice avalanche into the lake (Figs. 4 and 6)~~overall lake size~~. ~~Conversely, the resulting removal of the dam freeboard now leaves the lake more susceptible to an overtopping wave, caused by a potential ice avalanche or instability of the lateral moraine wall.~~ On the one hand, the engineering work has reduced the amount of moraine material available for initial erosion (leading to a more rapid and slowly attenuating water-dominated flow), while on the other hand, the reduction in freeboard has left the lake more susceptible to overtopping, resulting in a larger volume GLOF event (Fig 4a). ~~In general, increasing exposure of people and assets is seen as a main driver of disaster risk in mountain regions (Hock *et al.*, 2019), and this is clearly evidenced through the rapid increase in built infrastructure upstream of Nyalam over a two-year period, directly within the high intensity zone of potential GLOF paths (Fig. 6). Significant and permanent lowering of the water level in Jialongco would reduce the threat to these buildings from an outburst from this lake, but similar action would need to be repeated at Galongco and as new lakes emerge in the future, in order to minimise potentially larger, albeit, lower probability threats.~~The simulations also reveal the limited potential for early warning in the case of large process chains, with catastrophic GLOF discharges reaching Nyalam in only 5 – 11 minutes following an ice and/or rock avalanche detaching. For downstream communities in Nepal, warning times under worst-case scenarios could be as little as 30 minutes, which is a significant reduction on current estimates of up to 2 hours in the case of Galongco, whereby a more gradual lake breaching mechanism was modeled (Zhang *et al.* 2021). Particularly in transboundary regions requiring communication and collaboration between countries before any alert is acted upon, minutes lost or gained can be critical for effective early warning and evacuation.

Given the demonstrated minimal effect that lake lowering would have on a potentially devastating, worst-case GLOF from Jialongco, and the fact that warning times for all 3 assessed process chains would be minimal in Nyalam, w~~W~~e ~~would therefore~~ argue that a focus on engineering measures and early warning systems needs to be coupled with effective land use zoning and programs to strengthen local response capacities ~~capacity building programs (e.g., Huggel *et al.*, 2020),~~ (e.g., Huggel *et al.*, 2020). Such a comprehensive strategy would ~~provide a more effective, ecologically responsible, and forward looking response strategy,~~ reduc~~ing~~e the risk not only from an outburst from Jialongco, but also provide future-proofing against larger outburst scenarios from Galongco or potential new lakes that ~~may~~ develop ~~in the future~~over the next century. In general, increasing exposure of people and assets is seen as a main driver of disaster risk in mountain regions (Hock *et al.*, 2019), and this is clearly evidenced through the rapid increase in built infrastructure upstream of Nyalam, directly within the high-intensity zone of potential worst-case GLOF events (Fig. 6), but also within the path of more moderate events (Zhang *et al.* 2021). Lowering of the water level in Jialongco has likely reduced the threat to these buildings from a smaller, higher probability outburst event, but similar action would need to be repeated at Galongco and as new lakes emerge in the future, in order to maintain this minimum level of protection, while doing little to reduce the risk of a larger worst-case event. Land use zoning is therefore urgently required, in order to regulate the future development of infrastructure occurring within high hazard zones, also considering worst-case scenarios. GAPHAZ (2017) draws on the example of Switzerland, where very low probability events are included within a zone of "residual danger" that extends to include events with a return period of up to 300 years. At the least, evacuation centres and other critical infrastructure (e.g. schools, police, medical facilities), should be positioned well out of the potential inundated area. Furthermore, framing any EWS within a broader catchment-scale monitoring program could enable a degree of forecasting, allowing alert levels to be raised and evacuation~~s~~ preparations then ~~initated~~initiated within high hazard zones, prior to a warning system being activated. For example, precursory movement ~~assosciated~~associated with recent large high mountain slope failures has been detected with optical or InSAR satellite data (Carla *et al.* 2019; Bhardwaj and Sam 2021), and through dense seismic monitoring networks (Tiwari *et al.* 2022), although real-time operational monitoring systems are rare~~.~~ and should remain an important research priority.

~~Likewise for early warning, simulations show that warning times could be reduced by up to 20 minutes for downstream communities in Nepal, under a future outburst scenario. Hence, in order to ensure warning systems and response strategies remain robust over the longer term, it is recommended that authorities consider such future scenarios in the design phase, under the philosophy of preparing for the worst, while hoping for the best. Particularly in complex transboundary regions requiring communication and collaboration between countries, minutes lost or gained can be critical for effective early warning and evacuation.~~

While GlabTop and other similar modelling approaches (see Farinotti *et al.*, 2019a) have been widely used to anticipate future glacial lake locations and assess related risks and opportunities (e.g., Farinotti *et al.*, 2019b; Haeberli *et al.*, 2016a; Magnin *et al.*, 2015), large uncertainties remain as to if and when specific overdeepenings will transition into lakes. In this study, we have focussed on a very large overdeepening positioned beneath a flat, heavily debris-covered glacier tongue – a classic geomorphological setting in which large proglacial lakes typically develop (Benn *et al.*, 2012; Haritashya *et al.*, 2018), and analogous to the setting of Galongco. Coupled with the fact that conditions at the surface of the glacier have already allowed supraglacial lakes to form in the ablation zone of the glacier, there can be a high degree of confidence that a future proglacial lake will develop in this location, trapped behind the prominent terminal moraine. ~~The extrapolation of measured thinning rates over the glacier (Fig. 7) allowed for the estimation of when a glacial lake may begin to develop within the boundary of~~

~~the overdeepening beneath the glacier (Fig. 8). If the acceleration in thinning of the glacier which has occurred over the last four decades is replicated by 2100 (Scenario 1), or over an equivalent time period to that examined by King *et al.* (2019) (1974-2015- Scenario 2), 0.6-1.3 km^2 of the glaciers surface will sit below the hydrological base level of the glacier and therefore will likely host supraglacial meltwater.~~ Under ~~scenario 1,~~the two thinning scenarios employed in this study, supraglacial lake area equivalent to the current area of Jialongco will be replicated on glacier RGI60-15.09475 by ~2070 to 2100~~, and by ~2067 under scenario 2~~ (Fig. 8). These ~~two scenarios of thinning~~estimates may still represent a conservatively slower trajectory of lake development on this glacier. Both the development of extensive supraglacial ponds and ice cliff networks and the transition of a supraglacial lake to a full depth proglacial lake can increase the overall thinning rate in the ablation zone of debris-covered glaciers (King *et al.*, 2020; Mölg *et al.*, 2020; Thompson *et al.*, 2016). Our simple extrapolation of current thinning rates and patterns does not account for the initiation or expansion of these ablative processes. Therefore, we would rather expect greater thinning than our results predict in the lowermost ~1.5 km of the glacier over coming decades once a substantial amount of meltwater has ponded at the glaciers surface.

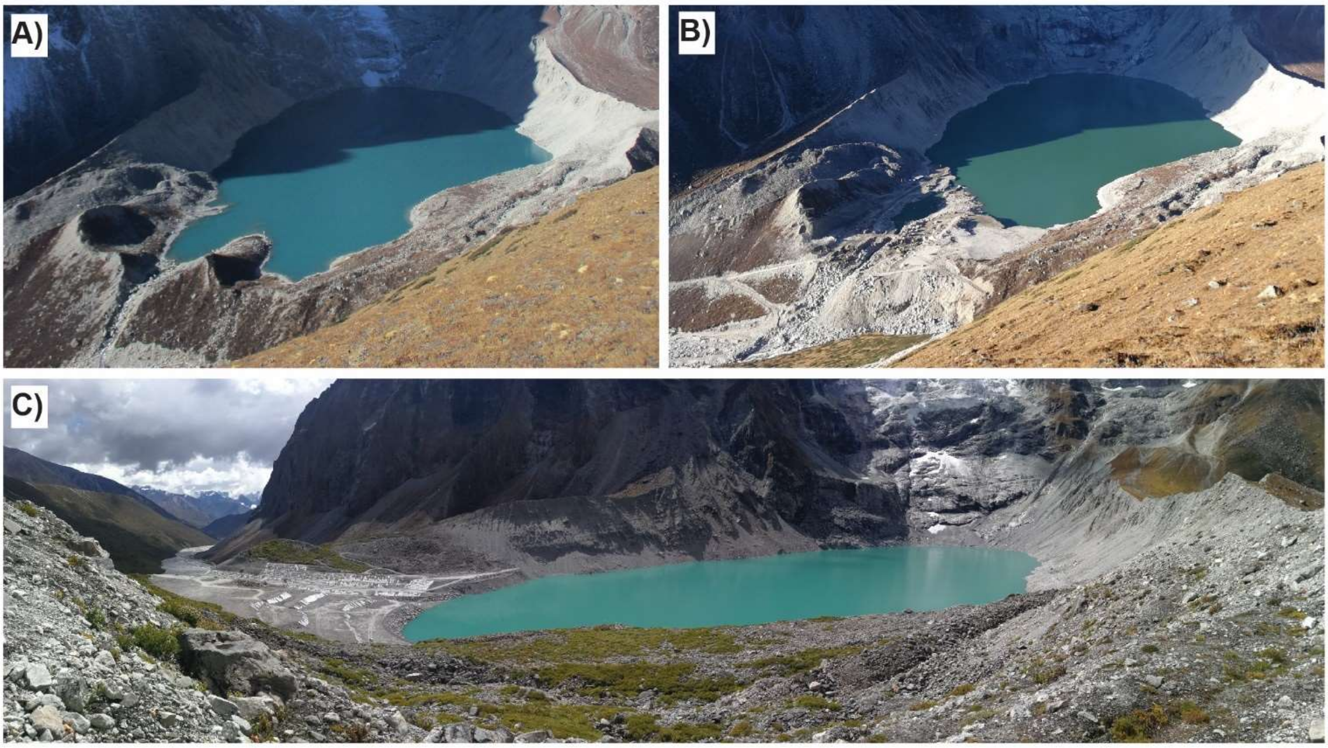

Figure 9: Images taken of Jialongco in A) October 2018 showing the natural state of the lake, ~~and~~ B) October 2020 and C) September 2021, ~~clearly~~ showing the engineering work that has been undertaken in the outlet area ~~of the lake~~, lowering the lake level, removing much of the frontal moraine, and establishing a stable, armoured outlet channel. Photos: T. Bolch (A) and G. Zhang (B, C).

Regardless of uncertainties in the timing of future lake development, ~~In general, the~~the results from this study suggest that hazard mapping and ~~land use planning~~associated response planning that accounts for existing worst-case outburst threats from Jialongco, and particularly Galongco, would largely remain valid for the future lake scenario. ~~, given only small differences in the potential built area affected (Fig. 6).~~ In other words, the potential magnitude of a worst-case GLOF from Galongco far exceeds anything the future lake could produce, while a worst-case event from Jialongco has the fastest arrival time in Nyalam. However, the formation of the new lake, and others, will undoubtedly increase the likelihood of a high magnitude event occurring within the basin, and hence, risk levels to people and infrastructure will increase if response strategies are not adequate. One of the key challenges in glacial hazard research is assigning a likelihood or probability to outburst scenarios, particularly for such very large scenarios for which there may be no historical precedence in a given basin (Allen *et al.* 2021). The worst-case scenarios modelled here are an order of magnitude larger than observed or assessed under previous studies (Shrestha *et al.* 2010, Zhang *et al.* 2021), but consider for the first time potential process chains involving large rock/ice avalanches > 20 million m^3 striking glacial lakes. The resulting GLOF discharges and flow heights produced by such catastrophic process chains modelled here are certainly extreme, with a return period exceeding 200 years relative to documented discharge values from past GLOFs in Asia (Carrivick *et al.* 2016).~~,~~ However, the recent Chamoli disaster, and earlier events from Seti River, remind that large avalanches capable of triggering such a process chain in the Himalaya do occur (Shugar *et al.* 2021), and their frequency is expected to be increasing as permafrost warms and slopes destabilise (Haeberli *et al.*, 2016b). Combined with larger and more numerous lakes (Zheng *et al.*, 2021b), the likelihood of high~~-~~-magnitude process chains occurring must be increasing over time, and therefore these more extreme scenarios need to be considered under a comprehensive approach to risk management. ~~despite uncertainties in the potential speed of future lake development, the opportunity cost of extending hazard zones and related planning to include areas potentially affected under future scenarios is minimal, particularly when considering the protection of critical infrastructure and services.~~

5 Conclusions

The Poiqu basin in the central Himalaya has been well established as a hotspot from which transboundary GLOF threats can originate. In the current study, we have focused on two lakes that directly threaten the Tibetan town of Nyalam and areas downstream, comparing the likelihood, potential magnitude, and impacts of large outburst events from these lakes. In addition, a future scenario has been modelled, whereby an outburst was simulated for a potential new lake, anticipated to form upstream of Jialongco. For all lakes, worst-case scenarios were ~~simulated~~assessed, ~~assuming release of the full potential flood volume of the lake as defined by the maximum breach height of the moraines~~with large rock and/or ice avalanches striking the lakes to trigger GLOF process chains. The study has recognised that:

- Jialongco, although smaller in size, poses the ~~greatest current~~most immediate threat to Nyalam and downstream communities, owing to ~~the high potential for an ice avalanche to trigger an outburst~~its position beneath a steep, heavily crevassed glacier tongue, and history of outburst events~~, feasibly leading to release of the full potential flood volume~~. Even though recent engineering work has ~~started the threat persists as the lake volume remains large and the reduced dam freeboard now leaves the lake more susceptible to an overtopping wave~~lowered the lake level by an average of 16 metres and stabilised the dam area, this has minimal effect on the magnitude and arrival time of a simulated worst-case GLOF triggered by a large ice avalanche.
- The likelihood of a~~An~~ large rock/ice avalanche >20 mil m^3 striking Galongco is considered very low, but increasing as permafrost slopes warm. The process chain would generate extreme GLOF discharges up to 5 times larger than simulated for Jialongco, resulting in flow heights up to 14 and 17 metres higher in Nyalam and at the border with Nepal (Zhangmu) respectively. ~~on its own is considered unlikely to initiate a large outburst from Galongco, although a low-probability/high impact event involving a catastrophic rock/ice avalanche into the lake should be considered as a realistic scenario, particularly given the seismic activity in the region.~~
- The assessed future lake could obtain a size comparable to Jialongco by 2070, but possibly earlier as a result of ablative processes around supraglacial ponds and ice cliffs on the debris-covered tongue. ~~A future scenario, involving~~

~~the anticipated new lake would lead to flow depths and velocities in Nyalam that exceed either of the current lakes, and the peak wave would reach the border with Nepal up to 20 minutes faster than for the current lakes.~~Even once the lake obtains its full potential area and volume, a worst-case rock avalanche-triggered outburst will have peak discharges and flow heights that are an order of magnitude lower than what Galongco can produce, but larger than for Jialongco.

- For all three assessed lakes, worst-case outburst events would impact Nyalam within 5-11 minutes of the process chain initiating, while reaching Zhangmu in around 30 minutes, posing severe challenges for early warning and evacuation.
- While previous studies have focused on rapid lake expansion in the region, for the town of Nyalam, it is rather the expansion of infrastructure directly within the high-intensity flood zone from both current and future lakes that has significantly increased GLOF ~~risk~~ exposure levels.

On the basis of these findings, a comprehensive and forward-looking approach to disaster risk reduction is called for, ~~combining~~ including early warning systems~~ with~~ , effective land use zoning and programs to build local response capacities~~capacity building programs~~. Relying only on h~~H~~ard engineering strategies ~~that address only the hazard~~at the lake source ~~are a socially and environmentally less desirable option~~will prove insufficient, as such strategies do ~~nothing to~~not address underlying ~~risk drivers of~~ exposure and vulnerability to GLOFS and other geohazards, and are ~~likely~~ demonstrated to be ~~unsustainable in the face of ongoing environmental changes~~ineffective in the face of worst-case, catastrophic outburst events.

Author contribution

SA and AS designed the study and undertook the GLOF modelling, and hazard assessment. OK performed the modelling of future lake development. AB produced the high resolution Pleiades DEM. SA, OK, TB, and GZ provided insights, images and bathymetry data from field visits. All authors contributed to the drafting of the manuscript and funding acquisition.

Acknowledgement

This work was supported by the Swiss National Science Foundation (IZLCZ2_169979/1). The work further benefited from support of the Strategic Priority Research Program of the Chinese Academy of Sciences (XDA20060201). We thank the two anonymous reviewers and Fabian Walter for their extremely comprehensive and constructive comments.

Competing interests

The authors declare that they have no conflict of interest.

References

Allen SK, Linsbauer A, Randhawa SS, Huggel C, Rana P, Kumari A. 2016. Glacial lake outburst flood risk in Himachal Pradesh, India: an integrative and anticipatory approach considering current and future threats. *Natural Hazards*. Springer Netherlands **84**(3): 1741–1763. DOI: 10.1007/s11069-016-2511-x.

Allen SK, Zhang G, Wang W, Yao T, Bolch T. 2019. Potentially dangerous glacial lakes across the Tibetan Plateau revealed using a large-scale automated assessment approach. *Science Bulletin*. Elsevier B.V. **64**(7): 435–445. DOI: 10.1016/j.scib.2019.03.011.

Allen, SK, Frey, H, Haeberli, W, Huggel, C, Chiarle, M, Geertsema, M. 2022. Assessment Principles for Glacier and Permafrost Hazards in Mountain Regions. *Oxford Research Encyclopedias: Natural Hazard Science.* https://doi.org/10.1093/acrefore/9780199389407.013.356

Benn DI, Bolch T, Hands K, Gulley J, Luckman A, Nicholson LI, Quincey D, Thompson S, Toumi R, Wiseman S. 2012. Response of debris-covered glaciers in the Mount Everest region to recent warming, and implications for outburst flood hazards. *Earth Science Reviews* **114**: 156–174.

Bhardwaj, A and Sam, L. 2022. Reconstruction and Characterisation of Past and the Most Recent Slope Failure Events at the 2021 Rock-Ice Avalanche Site in Chamoli, Indian Himalaya. *Remote Sensing,* **14** (4), 949, https://doi.org/10.3390/rs14040949

Bhattacharya A, Bolch T, Mukherjee K, King O, Menounos B, Kapitsa V, Neckel N, Yang W, Yao T. 2021. High Mountain Asian glacier response to climate revealed by multi-temporal satellite observations since the 1960s. *Nature Communications* in review.

Bolch T, Shea JM, Liu S, Azam FM, Gao Y, Gruber S, Immerzeel WW, Kulkarni A, Li H, Tahir AA, Zhang G, Zhang Y. 2019. Status and Change of the Cryosphere in the Extended Hindu Kush Himalaya Region. In: P. W, A. M, A. M and A. S (eds) *The Hindu Kush Himalaya Assessment*. Springer International Publishing: Cham, 209–255. DOI: 10.1007/978-3-319-92288-1_7.

Bolch T, Yao T, Bhattacharya A, Hu Y, King O, Liu L, Pronk JB, Rastner P, Zhang G. 2002. Earth Observation to Investigate Occurrence, Characteristics and Changes of Glaciers, Glacial Lakes and Rock Glaciers in the Poiqu River Basin (Central Himalaya). *Remote Sensing*, **14**(8):1927, https://doi.org/10.3390/rs14081927

Carlà, T, Intrieri, E, Raspini, F, Bardi, F, Farina, P, Ferretti, A, Colombo, D, Novali, F, Casagli, N. 2019. Perspectives on the prediction of catastrophic slope failures from satellite InSAR. *Scientific Reports*, **9** (1), 14137. https://doi.org/10.1038/s41598-019-50792-y.

Carrivick JL, Tweed FS. 2016. A global assessment of the societal impacts of glacier outburst floods. *Global and Planetary Change*. Elsevier B.V. **144**: 1–16. DOI: 10.1016/j.gloplacha.2016.07.001.

Chen NS, Hu GS, Deng W, Khanal N, Zhu YH, Han D. 2013. On the water hazards in the trans-boundary Kosi River basin. *Natural Hazards and Earth System Science* **13**(3): 795–808. DOI: 10.5194/nhess-13-795-2013.

Clague JJ, Evans SG. 2000. A review of catastrophic drainage of moraine-dammed lakes in British Columbia. *Quaternary Science Reviews* **19**: 1763–1783.

Cook KL, Andermann C, Gimbert F, Adhikari BR, Hovius N. 2018. Glacial lake outburst floods as drivers of fluvial erosion in the Himalaya. *Science (New York, N.Y.)*. American Association for the Advancement of Science **362**(6410): 53–57. DOI: 10.1126/science.aat4981.

Cook SJ, Quincey DJ. 2015. Estimating the volume of Alpine glacial lakes. *Earth Surface Dynamics* **3**(4): 559–575. DOI: 10.5194/esurf-3-559-2015.

Emmer A, Cochachin A. 2013. The causes and mechanisms of moraine-dammed lake failures in the Cordillera Blanca, North American Cordillera, and Himalayas. *AUC Geographica* **48**: 5–15.

Emmer A, Harrison S, Mergili M, Allen S, Frey H, Huggel C. 2020. 70 years of lake evolution and glacial lake outburst floods in the Cordillera Blanca (Peru) and implications for the future. *Geomorphology*. Elsevier B.V. **365**: 107178. DOI: 10.1016/j.geomorph.2020.107178.

Farinotti D, Huss M, Fürst JJ, Landmann J, Machguth H, Maussion F, Pandit A. 2019a. A consensus estimate for the ice thickness distribution of all glaciers on Earth. *Nature Geoscience*. Nature Publishing Group **12**(3): 168–173. DOI: 10.1038/s41561-019-0300-3.

Farinotti D, Round V, Huss M, Compagno L, Zekollari H. 2019b. Large hydropower and water-storage potential in future glacier-free basins. *Nature*. Springer US **575**(7782): 341–344. DOI: 10.1038/s41586-019-1740-z.

Frey H;, Huggel C;, Chisolm RE;, Baer P;, Mcardell BW;, Cochachin A;, Portocarrero. 2018. Multi-source glacial lake outburst flood hazard assessment and mapping for Huaraz, Cordillera Blanca, Peru. . DOI: 10.3389/feart.2018.00210.

Frey H, Haeberli W, Linsbauer A, Huggel C, Paul F. 2010. A multi-level strategy for anticipating future glacier lake formation and associated hazard potentials. *Natural Hazards and Earth System Sciences* **10**: 339–352.

~~Froehlich DC. 1995. Peak Outflow from Breached Embankment Dam. *Journal of Water Resources Planning and Management*. Publ by ASCE **121**(1): 90–97. DOI: 10.1061/(ASCE)0733-9496(1995)121:1(90).~~

Fujita K, Sakai A, Takenaka S, Nuimura T, Surazakov AB, Sawagaki T, Yamanokuchi T. 2013. Potential flood volume of Himalayan glacial lakes. *Natural Hazards and Earth System Science* **13**(7): 1827–1839. DOI: 10.5194/nhess-13-1827-2013.

Furian W, Loibl D, Schneider C. 2021. Future glacial lakes in High Mountain Asia: an inventory and assessment of hazard potential from surrounding slopes. *Journal of Glaciology*. Cambridge University Press (CUP) 1–18. DOI: 10.1017/jog.2021.18.

GAPHAZ. 2017. *Assessment of Glacier and Permafrost Hazards in Mountain Regions: Technical Guidance Document*. Standing Group on Glacier and Permafrost Hazards in Mountains (GAPHAZ) of the International Association of Cryospheric Sciences (IACS) and the International Permafrost Association (IPA). Zurich, Switzerland / Lima, Peru.

Gardelle J, Arnaud Y, Berthier E. 2011. Contrasted evolution of glacial lakes along the Hindu Kush Himalaya mountain range between 1990 and 2009. *Global and Planetary Change* **75**: 47–55.

Haeberli W, Buetler M, Huggel C, Lehmann Friedli T, Schaub Y, Schleiss AJ. 2016a. New lakes in deglaciating high-mountain regions – opportunities and risks. *Climatic Change* **139**: 201–214.

Haeberli W, Schaub Y, Huggel C. 2016b. Increasing risks related to landslides from degrading permafrost into new lakes in de-glaciating mountain ranges. *Geomorphology* doi: 10.1016/j.geomorph.2016.02.009.

Haritashya UK, Kargel JS, Shugar DH, Leonard GJ, Strattman K, Watson CS, Shean D, Harrison S, Mandli KT, Regmi D. 2018. Evolution and controls of large glacial lakes in the Nepal Himalaya. *Remote Sensing* **10**(5): 1–31. DOI: 10.3390/rs10050798.

~~Harrison S, Kargel JS, Huggel C, Reynolds J, Shugar DH, Betts RA, Emmer A, Glasser N, Haritashya UK, Klimeš J, Reinhardt L, Schaub Y, Wiltshire A, Regmi D, Vilímek V. 2018. Climate change and the global pattern of moraine-dammed glacial lake outburst floods. *The Cryosphere* **12**(4): 1195–1209. DOI: 10.5194/tc-12-1195-2018.~~

Hock R, Rasul G, Adler C, Cáceres B, Gruber S, Hirabayashi Y, Jackson M, Kääb A, Kang S, Kutuzov S, Milner A, Molau U, Morin S, Orlove B, Steltzer H. 2019. *High Mountain Areas. In: IPCC Special Report on the Ocean* *and Cryosphere in a Changing Climate [H.-O. Pörtner, D.C. Roberts, V. Masson-Delmotte, P. Zhai, M. Tignor, E. Poloczanska, K. Mintenbeck, A. Alegría, M. Nicolai, A. Okem, J. Petzold, B. Rama, N.M.* .

Huggel C, Cochachin A, Drenkhan F, Fluixá-Sanmartín J, Frey H, García Hernández J, Jurt C, Muñoz R, Price K, Vicuña L. 2020. Glacier Lake 513, Peru: lessons for early warning service development. *WMO Bulletin* **69**(1): 45–52.

Huggel C, Haeberli W, Kääb A, Bieri D, Richardson S. 2004. An assessment procedure for glacial hazards in the Swiss Alps. *Canadian Geotechnical Journal* **41**: 1068–1083.

Kääb A, Jacquemart M, Gilbert A, Leinss S, Girod L, Huggel C, Falaschi D, Ugalde F, Petrakov D, Chernomorets S, Dokukin M, Paul F, Gascoin S, Berthier E, Kargel JS. 2021. Sudden large-volume detachments of low-angle mountain glaciers – more frequent than thought? *The Cryosphere* **15**(4): 1751–1785. DOI: 10.5194/tc-15-1751-2021.

Khanal NR, Hu J-M, Mool P. 2015a. Glacial Lake Outburst Flood Risk in the Poiqu/Bhote Koshi/Sun Koshi River Basin in the Central Himalayas. *Mountain Research and Development* **35**: 351–364.

Khanal NR, Mool PK, Shrestha AB, Rasul G, Ghimire PK, Shrestha RB, Joshi SP. 2015b. A comprehensive approach and methods for glacial lake outburst flood risk assessment, with examples from Nepal and the transboundary area. *International Journal of Water Resources Development* **31**: 219–237.

King O, Bhattacharya A, Bhambri R, Bolch T. 2019. Glacial lakes exacerbate Himalayan glacier mass loss. *Scientific Reports*. Nature Research **9**(1). DOI: 10.1038/s41598-019-53733-x.

King O, Bhattacharya A, Ghuffar S, Tait A, Guilford S, Elmore AC, Bolch T. 2020. Six Decades of Glacier Mass Changes around Mt. Everest Are Revealed by Historical and Contemporary Images. *One Earth*. Cell Press **3**(5): 608–620. DOI: 10.1016/j.oneear.2020.10.019.

King O, Dehecq A, Quincey D, Carrivick J. 2018. Contrasting geometric and dynamic evolution of lake and land-terminating glaciers in the central Himalaya. *Global and Planetary Change*. Elsevier B.V. **167**: 46–60. DOI: 10.1016/j.gloplacha.2018.05.006.

~~Klimeš J, Novotný J, Novotná I, de Urries BJ, Vilímek V, Emmer A, Strozzi T, Kusák M, Rapre AC, Hartvich F, Frey H. 2016. Landslides in moraines as triggers of glacial lake outburst floods: example from Palcacocha Lake (Cordillera Blanca, Peru). *Landslides*. Springer Verlag **13**(6): 1461–1477. DOI: 10.1007/s10346-016-0724-4.~~

Korup O, Tweed F. 2007. Ice, moraine, and landslide dams in mountainous terrain. *Quarternary Science Reviews* **26**: 3406–3422.

Kraaijenbrink PDA, Bierkens MFP, Lutz AF, Immerzeel WW. 2017. Impact of a global temperature rise of 1.5 degrees Celsius on Asia's glaciers. *Nature Publishing Group* **549**: 5–7. DOI: 10.1038/nature23878.

Linsbauer A, Frey H, Haeberli W, Machguth H, Azam MF, Allen S. 2016. Modelling glacier-bed overdeepenings and possible future lakes for the glaciers in the Himalaya–Karakoram region. *Annals of Glaciology* **57**: 119–130.

Linsbauer A, Paul F, Haeberli W. 2012. Modeling glacier thickness distribution and bed topography over entire mountain ranges with GlabTop: application of a fast and robust approach. *Journal of Geophysical Research* **117**: doi: 10.1029/2011JF002313.

Linsbauer A, Paul F, Machguth H, Haeberli W. 2013. Comparing three different methods to model scenarios of future glacier change in the Swiss Alps. *Annals of Glaciology* **54**: 241–253.

Liu J-J, Tang C, Cheng Z-L. 2013. The Two Main Mechanisms of Glacier Lake Outburst Flood in Tibet, China. *J . Mt . Sci* **10**(2): 239–248. DOI: 10.1007/s11629-013-2517-8.

Lliboutry L, Morales AB, Pautre A, Schneider B. 1977. Glaciological problems set by the control of dangerous lakes in Cordillera Blanca, Peru. I. Historic failure of morainic dams, their causes and prevention. *Journal of Glaciology* **18**: 239–254.

Magnin F, Haeberli W, Linsbauer A, Deline P, Ravanel L. 2020. Estimating glacier-bed overdeepenings as possible sites of future lakes in the de-glaciating Mont Blanc massif (Western European Alps). *Geomorphology*. Elsevier B.V. **350**. DOI: 10.1016/j.geomorph.2019.106913.

Magnin F, Krautblatter M, Deline P, Ravanel L, Malet E, Bevington A. 2015. Determination of warm, sensitive permafrost areas in near-vertical rockwalls and evaluation of distributed models by electrical resistivity tomography. *Journal of Geophysical Research-Earth Surface* **120**: 745–762.

Maurer JM, Schaefer JM, Rupper S, Corley A. 2019. Acceleration of ice loss across the Himalayas over the past 40 years. *Science Advances*. American Association for the Advancement of Science **5**(6): eaav7266. DOI: 10.1126/sciadv.aav7266.

Mölg N, Ferguson J, Bolch T, Vieli A. 2020. On the influence of debris cover on glacier morphology: How high-relief structures evolve from smooth surfaces. *Geomorphology*. Elsevier B.V. **357**: 107092. DOI: 10.1016/j.geomorph.2020.107092.

Nie Y, Liu Q, Wang J, Zhang Y, Sheng Y, Liu S. 2018. An inventory of historical glacial lake outburst floods in the Himalayas based on remote sensing observations and geomorphological analysis. *Geomorphology*. Elsevier B.V. **308**: 91–106. DOI: 10.1016/j.geomorph.2018.02.002.

Nie Y, Sheng Y, Liu Q, Liu L, Liu S, Zhang Y, Song C. 2017. A regional-scale assessment of Himalayan glacial lake changes using satellite observations from 1990 to 2015. *Remote Sensing of Environment*. Elsevier Inc. **189**: 1–13. DOI: 10.1016/j.rse.2016.11.008.

~~Pozzi A, Stössel F, Zimmermann M. 2005. *Vademecum hazard maps and related instruments : the Swiss system and its application abroad : capitalisation of experiences*. Swiss Agency for Develpoment and Cooperation (SDC), Bern.~~

Pronk JB, Bolch T, King O, Wouters B, Benn DI. 2021. Proglacial Lakes Elevate Glacier Surface Velocities in the Himalayan Region. *The Cryosphere Discussions* in review. DOI: 10.5194/tc-2021-90.

Quincey DJ, Richardson SD, Luckman A, Lucas RM, Reynolds JM, Hambrey MJ, Glasser NF. 2007. Early recognition of glacial lake hazards in the Himalaya using remote sensing datasets. *Global and Planetary Change* **56**: 137–152.

Ren Y-Y, Ren G-Y, Sun X-B, Shrestha AB, You Q-L, Zhan Y-J, Rajbhandari R, Zhang P-F, Wen K-M. 2017. Observed changes in surface air temperature and precipitation in the Hindu Kush Himalayan region over the last 100-plus years. *Advances in Climate Change Research* **8**(3): 148–156. DOI: 10.1016/j.accre.2017.08.001.

Richardson SD, Reynolds JM. 2000. An overview of glacial hazards in the Himalayas. *Quaternary International* **65/66**: 31–47.

~~Romstad B, Harbitz CJ, Domaas U. 2009. A GIS method for assessment of rock slide tsunami hazard in all Norwegion lakes and reservoirs. *Natural Hazards and Earth System Sciences* **9**: 353–364.~~

Sanjay J, Krishnan R, Shrestha AB, Rajbhandari R, Ren GY. 2017. Downscaled climate change projections for the Hindu Kush Himalayan region using CORDEX South Asia regional climate models. *Advances in Climate Change Research*. National Climate Center **8**(3): 185–198. DOI: 10.1016/j.accre.2017.08.003.

Sattar A, Haritashya UK, Kargel JS, Leonard GJ, Shugar DH, Chase D V. 2021. Modeling Lake Outburst and Downstream Hazard Assessment of the Lower Barun Glacial Lake, Nepal Himalaya. *Journal of Hydrology*. Elsevier BV **598**: 126208. DOI: 10.1016/j.jhydrol.2021.126208.

Schaub Y, Huggel C, Cochachin A. 2015. Ice-avalanche scenario elaboration and uncertainty propagation in numerical simulation of rock-/ice-avalanche-induced impact waves at Mount Hualcán and Lake 513, Peru. *Landslides* doi:10.1007/s10346-015-0658-2.

Schmid M-O, Baral P, Gruber S, Shahi S, Shrestha T, Stumm D, Wester P. 2015. Assessment of permafrost distribution maps in the Hindu Kush Himalayan region using rock glaciers mapped in Google Earth. *The Cryosphere* **9**: 2089–2099.

Schneider D, Huggel C, Haeberli W, Kaitna R. 2011. Unraveling driving factors for large rock-ice avalanche mobility. *Earth Surface Processes and Landforms* **36**: 1948–1966.

Shedlock KM, Giardini D, Grünthal G, Zhang P. 2000. The GSHAP Global Seismic Hazard Map. *Seismological Research Letters*. Seismological Society of America **71**(6): 679–686. DOI: 10.1785/gssrl.71.6.679.

Shijin W, Shitai J. 2015. Evolution and outburst risk analysis of moraine-dammed lakes in the central Chinese Himalaya. *Journal of Earth System Science*. Springer India **124**(3): 567–576. DOI: 10.1007/s12040-015-0559-8.

Shrestha AB, Eriksson M, Mool P, Ghimire P, Mishra B, Khanal NR. 2010. Glacial lake outburst flood risk assessment of Sun Koshi basin, Nepal. *Geomatics, Natural Hazards and Risk*. Taylor & Francis **1**(2): 157–169. DOI: 10.1080/19475701003668968.

Shugar DH, Burr A, Haritashya UK, Kargel JS, Watson CS, Kennedy MC, Bevington AR, Betts RA, Harrison S, Strattman K. 2020. Rapid worldwide growth of glacial lakes since 1990. *Nature Climate Change*. Springer US **10**(10): 939–945. DOI: 10.1038/s41558-020-0855-4.

Thompson S, Benn DI, Mertes J, Luckman A. 2016. Stagnation and mass loss on a Himalayan debris-covered glacier: Processes, patterns and rates. *Journal of Glaciology*. International Glaciology Society **62**(233): 467–485. DOI: 10.1017/jog.2016.37.

Tiwari, A, Sain, K, Kumar, A, Tiwari, J, Paul, A, Kumar, N, Haldar, C, Kumar, S, Pandey, CP. 2022. Potential seismic precursors and surficial dynamics of a deadly Himalayan disaster: an early warning approach. *Scientific Reports*, **12**(1), 3733. https://doi.org/10.1038/s41598-022-07491-y

Veh G, Korup O, von Specht S, Roessner S, Walz A. 2019. Unchanged frequency of moraine-dammed glacial lake outburst floods in the Himalaya. *Nature Climate Change*. Nature Publishing Group, 379–383. DOI: 10.1038/s41558-019-0437-5.

Wang S, Dahe Q, Xiao C. 2015a. Moraine-dammed lake distribution and outburst flood risk in the Chinese Himalaya. *Journal of Glaciology* **61**: 115–126.

Wang S, Zhou L. 2017. Glacial Lake Outburst Flood Disasters and Integrated Risk Management in China. *International Journal of Disaster Risk Science* **8**. DOI: 10.1007/s13753-017-0152-7.

Wang W, Gao Y, Iribarren Anacona P, Lei Y, Xiang Y, Zhang G, Li S, Lu A. 2018. Integrated hazard assessment of Cirenmaco glacial lake in Zhangzangbo valley, Central Himalayas. *Geomorphology* http://dx.doi.org/10.1016/j.geomorph.2015.08.013.

Wang W, Xiang Y, Gao Y, Lu A, Yao T. 2015b. Rapid expansion of glacial lakes caused by climate and glacier retreat in the Central Himalayas. *Hydrological Processes*. John Wiley & Sons, Ltd **29**(6): 859–874. DOI: 10.1002/hyp.10199.

Westoby MJ, Glasser NF, Brasington J, Hambrey MJ, Quincey DJ, Reynolds JM. 2014. Modelling outburst floods from moraine-dammed glacial lakes. *Earth-Science Reviews* **134**: 137–159. DOI: http://dx.doi.org/10.1016/j.earscirev.2014.03.009.

Worni R, Stoffel M, Huggel C, Volz C, Casteller A, Luckman B. 2012. Analysis and dynamic modeling of a moraine failure and glacier lake outburst flood at Ventisquero Negro, Patagonian Andes (Argentina). *Journal of Hydrology* **444**–**445**: 134–145.

~~Xu D. 1988. Characteristics of debris flow caused by outburst of glacial lake in Boqu river, Xizang, China, 1981. *GeoJournal*. Kluwer Academic Publishers **17**(4): 569–580. DOI: 10.1007/BF00209443.~~

Zemp M, Huss M, Thibert E, Eckert N, McNabb R, Huber J, Barandun M, Machguth H, Nussbaumer SU, Gärtner-Roer I, Thomson L, Paul F, Maussion F, Kutuzov S, Cogley JG. 2019. Global glacier mass changes and their contributions to sea-level rise from 1961 to 2016. *Nature*. Nature Publishing Group, 382–386. DOI: 10.1038/s41586-019-1071-0.

Zhang G, Bolch T, Allen S, Linsbauer A, Chen W, Wang W. 2019. Glacial lake evolution and glacier–lake interactions in the Poiqu River basin, central Himalaya, 1964–2017. *Journal of Glaciology*. Cambridge University Press 1–19. DOI: 10.1017/jog.2019.13.

Zhang G, Yao T, Xie H, Wang W, Yang W. 2015. An inventory of glacial lakes in the Third Pole region and their changes in response to global warming. *Global and Planetary Change* **131**: 148–157.

Zhang, T, Wang, W, Gao, T. An, B. 2021. Simulation and Assessment of Future Glacial Lake Outburst Floods in the Poiqu River Basin, Central Himalayas. *Water*, **13**(1376), https://doi.org/10.3390/w13101376.

Zheng G, Allen SK, Bao A, Ballesteros-Cánovas JA, Huss M, Zhang G, Li L, Yuan Y, Jiang L, Yu T, Chen W, Stoffel M. 2021a. Increasing risk of glacial lake outburst floods from future Third Pole deglaciation. *Nature Climate Change* https://doi.org/10.1038/s41558-021-01028-3.

Zheng G, Mergili M, Emmer A, Allen S, Bao A, Guo H, Stoffel M. 2021b. The 2020 glacial lake outburst flood at Jinwuco, Tibet: causes, impacts, and implications for hazard and risk assessment. *The Cryosphere Discussions* 1–28. DOI: 10.5194/tc-2020-379.